

Current progress on catalytic oxidation of toluene: A review

David Murindababisha ¹, Abubakar Yusuf ¹, Yong Sun ^{1*}, Chengjun Wang ^{2*}, Yong Ren ³,
Jungang Lv ⁴, Hang Xiao ⁵, George Zheng Chen ⁶, Jun He ^{1,7*}

¹ *Department of Chemical and Environmental Engineering, University of Nottingham Ningbo China, Ningbo, China*

² *College of Resources and Environmental Science, South-Central University for Nationalities, Wuhan, China*

³ *Department of Mechanical, Materials and Manufacturing Engineering, University of Nottingham Ningbo China, Ningbo, China*

⁴ *Procuratorial Technology and Information Research Center, Supreme People's Procuratorate, Beijing, China*

⁵ *Centre for Excellence in Regional Atmospheric Environment, Institute of Urban Environment, Chinese Academy of Sciences, Xiamen, China*

⁶ *Department of Chemical and Environmental Engineering, Faculty of Engineering, University of Nottingham, Nottingham, UK*

⁷ *Key Laboratory of Carbonaceous Wastes Processing and Process Intensification Research of Zhejiang Province. University of Nottingham Ningbo China, Ningbo, China*

Correspondence authors:

Dr. Yong Sun, email: sun.yong@nottingham.edu.cn

Prof. Chengjun Wang, email: cjwang@scuec.edu.cn

Prof. Jun He, email: jun.he@nottingham.edu.cn

26 **Abstract**

27 Toluene is one of the pollutants that are dangerous to the environment and human health and has
28 been sorted into priority pollutants; hence the control of its emission is necessary. Due to severe
29 problems caused by toluene, different techniques for the abatement of toluene have been developed.
30 Catalytic oxidation is one of the promising methods and effective technologies for toluene
31 degradation as it oxidizes it to CO₂ and does not deliver other pollutants to the environment. This
32 paper highlights the recent progressive advancement of the catalysts for toluene oxidation. Five
33 categories of catalysts, including noble metal catalysts, transition metal catalysts, perovskite
34 catalysts, metal-organic framework (MOFs)-based catalysts, and spinel catalysts reported in the
35 past half a decade (2015-2020), are reviewed. Various factors that influence their catalytic
36 activities, such as morphology and structure, preparation methods, specific surface area, relative
37 humidity, and coke formation, are discussed. Furthermore, the reaction mechanisms and kinetics
38 for catalytic oxidation of toluene are also discussed.

39 **Keywords:** Toluene, catalysts, oxidation, catalytic performance.

40

41

42

43

44

45

46

47

48

49

50 **1. Introduction**

51 Toluene is a volatile organic compound (VOC) known to be harmful to human health and the
52 environment (Carrillo and Carriazo 2015; Liu et al. 2015; Narayanan et al. 2015; Romero et al.
53 2015). Naturally, toluene is found in tolu trees and crude oil. It is generated in some anthropogenic
54 activities like manufacturing processes of fuels and coke. It is commonly used in the production
55 processes of paint, adhesives, fingernail polish, rubber, and lacquers. It is also used in benzene,
56 plastics, nylon, and polyurethane production, and in the synthesis reaction of toluene diisocyanate,
57 benzoic acid, trinitrotoluene (TNT), and benzoyl chloride, thus playing a crucial role in daily
58 human life and industrial development for the past several decades (Zhang et al. 2019a). However,
59 due to its toxicity and volatility, toluene has been recorded in Pollutant Released and Transfer
60 Register (PRTR) in many countries (Nunotani et al. 2020).

61 The toluene concentration in ambient air is not the same in different areas. In rural areas, it has
62 been found generally to be $< 5 \mu\text{g}/\text{m}^3$, while in urban sites it could be in the range of 5 to 150
63 $\mu\text{g}/\text{m}^3$; but its concentration may be even higher in the areas closer to the emission sources (Bravo
64 et al. 2002). Exposure to toluene may cause serious health problems such as brain and nervous
65 system disorders that can be temporary, like dizziness, headaches, or unconsciousness. For
66 repeated exposure of the concentrations prohibited by international solvent, some effects like
67 vision and hearing loss, cognitive impairment, and incoordination may be permanent (Lerner et al.
68 2012). Long-term exposure for pregnant people can cause mental growth and abilities retardation
69 in children, and sometimes spontaneous abortions may take place. Other serious problems related
70 to human health may include liver, immune, reproductive, and kidney effects (Lerner et al. 2012).
71 Besides, toluene has been found to have carcinogenic, mutagenic, developmental, and teratogenic
72 effects on humans and animals. Toluene is also harmful to the environment, where it contributes
73 to the formation of photochemical smog, climate change, and destruction of the ozone layer (Zhang
74 et al. 2016; Xu et al. 2015b). Therefore, effective technologies to remove toluene from
75 contaminated gas streams are needed to improve the ambient air quality as well as to protect human
76 health.

77 From the literature, various approaches for abatement of toluene have been proposed and
78 reported, including thermal or non-thermal catalytic oxidation, adsorption (Hu et al. 2017; Uzuki
79 et al. 2018; Mekki and Boukoussa 2019; Song et al. 2019; Yin et al. 2019), and photocatalytic

80 oxidation, etc. (Mills and O'Rourke 2012; Sun et al. 2017; Qiu et al. 2018; Lee et al. 2019; Zhu et
81 al. 2019a; Xie et al. 2020). The adsorption process has been widely used due to the lowest cost,
82 simplicity to easy design and operation; however, it suffers from well-recognized restrictions,
83 including the limited adsorption capacity, relative humidity (RH) impact, and pollutants released
84 during regeneration of the material by desorption (Peta et al. 2018; Thanh et al. 2018a).
85 Photocatalytic oxidation has been applied for the abatement of toluene due to its advantages like a
86 wide range of applications, higher mineralization ability, lower oxidation temperature, simple
87 conditions to operate, and little secondary pollutants released (Li et al. 2020; Li & Ma 2021; Ezech
88 et al 2018); but it was reported to have drawbacks, which mainly include its high recombination
89 rate of holes and electrons or photons and the narrow overlap between the sunlight and
90 photocatalyst's absorption spectrum (Xie et al. 2020; Tomatis et al. 2016).

91 Toluene's catalytic oxidation has been widely used as an alternative solution due to its high
92 efficiency in removing toluene as it can convert it entirely to CO₂ and H₂O with no release of other
93 secondary pollutants to the environment (Hoseini et al. 2019; Zhang et al. 2019b). But in practical
94 application, this technique is still facing different challenges. One is synthesizing a catalyst that
95 can achieve 100% toluene conversion at a possible lower reaction temperature for energy saving.
96 Current catalytic technology for removing toluene and other VOCs from coal-fired flue gas is the
97 selective catalytic reduction with NH₃ (NH₃-SCR), which normally uses the V₂O₅-WO₃/TiO₂
98 catalysts but needs high temperature above 340 °C and the efficiency for the oxidation of VOCs
99 is still lower than 50% (Wu et al. 2016; Han et al. 2019). During the industrial process
100 implementation, energy is the first issue to think about, especially for the treatment of exhaust
101 gases (Gan et al. 2019). Efficient thermal catalysts can lower the operating temperatures to save
102 the auxiliary fuel consumption and the need for advanced thermal insulation or thermally stable
103 construction materials (Tomatis et al., 2019). Besides, the cost of a catalyst and its ability to tolerate
104 the moisture in the reaction atmosphere are also important factors to be taken into account for
105 practical uses. Up to the present, a significant number of active catalysts for toluene oxidation or
106 combustion have been reported, and it has seen that total oxidation of toluene can be achieved
107 catalytically at low temperature (Torrente-murciano et al. 2017; Zhu et al. 2018a) and even at room
108 temperature (Liu et al. 2015; Ryu et al. 2019); thus it appears to be a promising technique for
109 removing toluene. Previous reviews of toluene's catalytic oxidation have commonly focused on
110 only one type of catalyst. For instance, Lyu et al. (2020) reviewed toluene catalytic removal, but

111 they focused only on Mn-based catalysts. Similarly, Zhang et al. (2015) reported catalytic
112 oxidation of toluene by focusing only on one type of catalyst (mesoporous silica-based catalysts).
113 Up to now, there is almost no article available that comprehensively reviewed various types of
114 catalysts used for thermal oxidation of toluene particularly in flue gases. The recent one was
115 reported by Cui et al. (2016) where they focused on the status and progress of treatment
116 technologies of toluene in the industrial waste gas; however, that article is with short English
117 abstract but the full paper is only available in the Chinese language, which makes it difficult to be
118 shared with the international research communities.

119 According to the reported literature, it can be easily seen that significant advancement in
120 catalytic oxidation of toluene has been done using different methods. Nevertheless, to the best of
121 our knowledge, no report has made on the review of catalytic oxidation techniques of toluene in
122 detail, considering different types of catalysts. Thus, this literature review will be beneficial to the
123 environmental researchers better to understand recent progress on catalytic oxidation of toluene.
124 Besides, it may further attract researchers' attention and encourage them to conduct studies on
125 toluene remediation technologies. This review emphasizes the current progressive research over a
126 half-decade on catalysts for toluene oxidation especially including noble metal-based catalysts,
127 transition metal-based catalysts, perovskite catalysts, metal-organic framework (MOFs)-based
128 catalysts, core-shell catalysts, and spinel catalysts; also, reaction mechanisms are summarized, and
129 future perspectives are identified.

130 **2. Noble metal-based catalysts**

131 Noble metal-based catalysts generally have better catalytic activity for toluene combustion than
132 transition metal oxides catalysts (Santos et al. 2010). Noble metals like platinum (Pt), palladium
133 (Pd), gold (Au), and silver (Ag) are commonly used in the toluene's catalytic oxidation, where
134 they work as active phases of the catalysts. These materials can be utilized as single metals or
135 bimetallic composites loaded on different supports, as is shown in Tables 1 and 2, and they have
136 been found to have the highest toluene oxidation activity at low temperatures, even less than
137 100 °C (Torrente-murciano et al. 2017; Zhu et al. 2018b). Nonetheless, noble metals are extremely
138 expensive with limited resources, and this will make noble metal-based catalysts costly, which will
139 be a limitation for their wide industrial application. Thus, to overcome this challenge, numerous
140 research efforts have been done to improve the catalyst by raising the spread of noble metals on

141 their supports through different preparation techniques. Therefore, the one-step synthesis method
142 could be a promising solution to increase the dispersion of active phases on the support during the
143 preparation of noble metal-based catalysts (Fu et al. 2016) as the traditional wet impregnation
144 method showed limitations in the doped particles' stabilization and distribution (Sun et al, 2019;
145 Debecker et al. 2010).

146 **2.1 Single noble metal-based catalysts**

147 **2.1.1 Platinum-based catalysts**

148 Pt-based catalysts are mostly used as monometallic catalysts supported on various supports for
149 toluene oxidation (Table 1). They show an excellent activity for the removal of toluene at reaction
150 temperatures ranging between 150 and 200 °C (Table 1). Pt has been found to be an excellent
151 active element for aromatic structure oxidation (Peng et al. 2016). Pt catalysts supported with
152 different supports, including zeolites, CeO₂, Al₂O₃, and molecular sieves, have been prepared and
153 tested for toluene oxidation (Chen et al. 2013; Peng et al. 2016; Gan et al. 2019). The size and
154 dispersion of Pt on the support surface significantly influence the catalyst activity. To study the
155 effect of Pt size on the catalytic activity, various sizes of Pt nanoparticles (1.3 to 2.5 nm) were
156 synthesized and loaded on CeO₂ as support. Structural and chemical properties were highly
157 depended on Pt size, and it was realized that the dispersion of Pt decreases with the increase of its
158 size. The prepared catalysts were tested on 1000ppm of toluene with 48000 mL•g⁻¹•h⁻¹ of GHSV.
159 Pt-1.8/CeO₂ exhibited better catalytic activity where it was able to reach T₅₀ and T₉₀ at 132 and
160 143 °C respectively, due to the balanced concentration of oxygen vacancy and dispersion of Pt
161 (Peng et al. 2018). Similarly, the role of Pt particle size for total toluene oxidation over Pt/ZSM-5
162 was investigated and various catalysts with different sizes (1.3-2.3 nm) of Pt particles were
163 synthesized and tested (Chen et al. 2015a). Of the tested catalysts, a catalyst of 1.9 nm of mean
164 particle diameter showed the highest performance where 98% of toluene conversion was observed
165 at 155 °C with gas hourly space velocity (GHSV) of 60,000 mL•g⁻¹•h⁻¹. The most increased activity
166 of Pt-1.9/ZSM-5 was ascribed to the balanced dispersion of Pt and the proportion of Pt⁰ in the
167 catalyst. To explain this, the relationship between Pt⁰ and Pt size was studied and it was found that
168 Pt⁰ proportion was increased with the size of Pt particle, which was ascribed to the interaction
169 between the active metal and support (An et al. 2013). Smaller nanoparticles of Pt could have

170 higher interaction with support which results in a high chemical state of Pt species. On the contrary,
171 larger nanoparticles of Pt have weak interaction with support, leading to the formation of more
172 species of Pt⁰ which are the active centers for the complete oxidation of toluene (Chen et al. 2014).
173 On another side, the dispersion of Pt strongly influences the activity of the catalyst. Again, the
174 dispersion of Pt is decreased with the increase of Pt size (Chen et al. 2015a). Thus, the balance
175 between the dispersion of Pt and the proportion of Pt⁰ can affect the catalytic activity of the catalyst.

176 Recently, zeolitic mesoporous materials were prepared to attempt the combination of zeolitic
177 and mesoporous properties (Kim et al. 2010). Pt particles were immobilized on the material surface
178 and tested for toluene destruction. Mesoporous beta zeolite-supported Pt was found to exhibit the
179 highest performance compared to the other catalysts synthesized on beta zeolite. The highest
180 activity was ascribed to the dispersion of Pt and the ratio of Pt⁰/Pt²⁺ (Chen et al. 2013). Pt⁰
181 proportion of Pt catalyst supported on mesoporous ZSM-5 could be enhanced by the doping of
182 alkali metals such as Na, Cs, and K, which could also ameliorate the activity of the catalyst (Chen
183 et al. 2015b).

184 The catalytic activity of Pt catalysts could be promoted by different dopants like tungsten as
185 reported by Hou et al. 2019, who studied the tungsten effect for promoting the toluene catalytic
186 activity of monolith Pt/Ce_{0.65}Zr_{0.35}O₂ and it was found that the incorporation of tungsten in
187 monolith Pt/Ce_{0.65}Zr_{0.35}O₂ facilitated the decrease of 30 °C to the required temperature for the
188 total conversion of toluene compared to the one needed by Pt/Ce_{0.65}Zr_{0.35}O₂ for degrading
189 1000ppm of toluene under 12000 h⁻¹ of GHSV. The best performance of this catalyst was due to
190 the increase of surface acidity and adsorbed oxygen caused by the addition of WO₃.

191 Toluene oxidation can also be catalytically affected by the shape of the support for Pt-based
192 catalyst. For instance, the shape effect of Pt/CeO₂ on toluene oxidation was investigated and three
193 different shapes of CeO₂ such as nanoparticles, nanorods and, nanocubes were used (Peng et al.
194 2016). It was found that the amount of Ce³⁺ is estimated to be 32.9%, 29.7% and 27.3% for
195 Pt/CeO₂-r, Pt/CeO₂-p and Pt/CeO₂-c, respectively. The high concentration of Ce³⁺ ions on the
196 surface of Pt/CeO₂-r sample reflects the high concentration of surface oxygen vacancies. For pure
197 CeO₂ supports, the reduction of surface or subsurface oxygen occurs with the maxima at 428 °C,
198 380 °C and 510 °C for CeO₂-r, CeO₂-p and CeO₂-c, respectively. And the total H₂ consumptions
199 follows such a sequence: CeO₂-r (718 μmol g⁻¹) > CeO₂-p (275 μmol g⁻¹) > CeO₂-c (89.6 μmol g⁻¹)

200 ¹), indicating that the reduction of CeO₂ is influenced significantly by the exposed shape. It also
201 indicated that more subsurface lattice oxygen of Pt/CeO₂-r had been reduced, which was probably
202 due to the spillover effect on the subsurface oxygen below the Pt species. The H₂-TPR study clearly
203 demonstrated that the incorporation of Pt would activate the lattice oxygen on surface/subsurface
204 of CeO₂ and promote the reducibility, especially for Pt/CeO₂-r. In the moisturized environment,
205 Pt-based catalysts are negatively affected by deactivation due to water adsorption on the support
206 (Sedjame et al. 2014). In some cases, the utilization of supports that are hydrophobic can be
207 advantageous as they can be involved in the expulsion of water vapor from the surfaces of the
208 catalyst.

209 From the reported research work, Pt catalysts have shown more activity at a lower temperature
210 compared to other noble metals catalysts for toluene oxidation. However, few studies have
211 reported the Pt effect on the active oxygen of the catalysts. For the exploration of their potentials,
212 further research can focus on the quantitative analysis and the improvement of active surface
213 oxygen by different dopants to increase the catalyst performance.

214 **2.1.2 Gold-based catalysts**

215 Au is less expensive compared to Pd and Pt. Au-based catalysts catalyze the oxidation of toluene
216 at a higher reaction temperature (200 - 400 °C), but under some circumstances, it can work at a
217 lower temperature (< 100 °C). For example, the removal of toluene using supported nano-
218 gold/metal oxides catalysts was investigated, and it was shown that the prepared gold-catalysts
219 (nano-Au/Fe₂O₃/GAC and nano-Au/CeO₂/GAC) were able to achieve toluene removal of 80% at
220 the reaction temperature of 75 °C (Thanh et al. 2018). There are different methods to synthesize
221 Au-based catalysts, such as chemical vapor deposition, deposition-precipitation, and cation
222 adsorption methods (Liotta 2014). From the literature, it has been found that compared to other
223 supports, gold catalysts supported on metal oxide supports showed excellent performance towards
224 toluene oxidation (Carabineiro et al. 2015; Sun et al. 2019a).

225 The catalytic performance of Au catalysts can be influenced by a few factors such as the types
226 of supports and the size of dispersed Au particles (Han et al. 2014). In one investigation, the
227 support effect on the performance of Au particles for the oxidation of toluene was studied where
228 MgO, Fe₂O₃, NiO, and La₂O₃ were used as supports to prepare gold-based catalysts, and it was

229 realized that the activity of the prepared catalyst was majorly affected by reducibility and the size
230 of the crystal while the gold oxidation state did not show any distinctive impact on the catalyst's
231 activity (Carabineiro et al. 2015). Catalysts of Au immobilized on 3DOM structured materials
232 were studied and it was found that 3DOM perovskite materials like LaSrCoO_x and LaSrMnO_x are
233 suitable supporting materials of Au particles due to their structured 3D pores and high surface area
234 (Jiang et al. 2017). In another separate study, Au catalyst supported on $\text{La}_{0.6}\text{Sr}_{0.4}\text{MnO}_3$ was
235 explored and the prepared catalyst showed excellent performance towards the oxidation of toluene
236 where the conversion of 50 and 90% were reached at a temperature of 205 and 220 °C, respectively
237 (Jiang et al. 2015).

238 Previous investigators have determined that the incorporation of transition metal oxides to
239 supported noble metal catalyst (SNMC) could enhance the catalytic activity for the oxidation of
240 VOC, and this was found to be the case for toluene oxidation. $\text{Au/MnO}_x/3\text{DOM SiO}_2$ as a highly
241 effective gold-based catalyst for the oxidation of toluene was studied and it was determined that
242 $\text{Mn}_x/3\text{DOM-SiO}_2$ and $\text{Au}/3\text{DOM-SiO}_2$ were less active than their corresponding
243 $\text{Au/MnO}_x/3\text{DOM-SiO}_2$ where the conversion of 90% was reached at 255 °C when GHSV and
244 toluene concentration were 20,000 $\text{mL}\cdot\text{g}^{-1}\cdot\text{h}^{-1}$ and 1000ppm respectively (Yang et al. 2015a).
245 Similarly, among the three prepared catalysts ($\text{Au}/3\text{DOM La}_{0.6}\text{Sr}_{0.4}\text{MnO}_3$, $\text{MnO}_x/3\text{DOM}$
246 $\text{La}_{0.6}\text{Sr}_{0.4}\text{MnO}_3$ and $\text{Au/MnO}_x/3\text{DOM La}_{0.6}\text{Sr}_{0.4}\text{MnO}_3$) under the same reaction conditions (GHSV
247 of 20,000 $\text{mL}\cdot\text{g}^{-1}\cdot\text{h}^{-1}$ and toluene concentration of 1000ppm), $\text{Au/MnO}_x/3\text{DOM La}_{0.6}\text{Sr}_{0.4}\text{MnO}_3$
248 nanocatalyst showed the highest activity for total toluene oxidation ($T_{50} = 205$ °C and $T_{90} = 220$ °C)
249 due to its larger surface area, high concentration of adsorbed oxygen, and powerful interaction of
250 Au nanoparticles or Manganese oxides and 3DOM LSMO (Jiang et al. 2015). A gold-based
251 catalyst supported on mesoporous ferrisilicates (MFS) was also synthesized for total oxidation of
252 toluene and the results showed that the complete toluene oxidation achieved at 374 °C, and the
253 catalytic activity of the catalyst increased with the iron content (Benais-Hamidi et al. 2015).

254 A literature search showed the absence of coke formation as a byproduct of incomplete
255 combustion of toluene. However, the reported works on the utilization of Au catalysts at a lower
256 temperature are still scarce. Therefore, more studies are required to find out the potential of Au-
257 based-catalyst that can help the oxidation of toluene at a lower temperature. Furthermore, other

258 research can focus on other dopants that can help Au to create more surface-active oxygen on the
259 catalyst to increase its activity at a lower reaction temperature.

260 **2.1.3 Palladium-based catalysts**

261 Pd catalysts are used for the oxidation of toluene and exhibit high thermal and hydrothermal
262 resistance compared to the rest of the noble metals-based catalysts (Huang et al. 2008). Pd catalysts
263 supported on different supports like metal oxides and porous silica have been shown to have high
264 activity for this kind of reaction. Their highest performance has been attributed to a dual role of
265 Pd where Pd metal sites are active for the degradation of toluene and PdO supplies an extra source
266 of oxygen on the surface. Besides, Pd supported catalysts are more stable than Pt-supported
267 catalysts for toluene degradation (Liu et al. 2013).

268 Porous silica has been reported as good support of Pd nanoparticles and ZSM-5 was found to
269 be stable and coke-resistant for Pd supported catalysts. In this case, the dispersion of Pd and redox
270 potential can be influenced by the acidity of support (He et al. 2012a). The quantitative moles of
271 the acid sites, corresponding to the amounts of adsorbed ammonia measured by NH₃-TPD, were
272 positively correlated with the improved dispersion and accelerated oxidation of Pd, both of which
273 had the cumulative effects on toluene oxidation. The importance of acidic sites of zeolite was to
274 anchor the dispersed form of PdO (He et al. 2014). It was found that the main role of zeolite's
275 protons is to maintain Pd²⁺ formed through the reaction between PdO particles and zeolite protons
276 to form Pd²⁺ cations ($\text{PdO} + 2\text{H}^+ \rightarrow \text{Pd}^{2+} + \text{H}_2\text{O}$) (Okumura et al. 2000). To understand the effect
277 of acidity on the catalytic performance of the catalysts, the catalyst's acidic properties were
278 explored and it was found that the increase of acidity on the surfaces of the catalyst facilitates the
279 oxidation of toluene (Hou et al. 2019). To explain this, possible pathways for the degradation of
280 toluene were investigated and showed the adsorption of toluene to take place first, followed by its
281 oxidation to benzaldehyde, benzoic acid then undergoes the formation of small molecules
282 (carbonates and carboxylates) and end up with CO₂ and H₂O production (Rui et al. 2017). Since
283 carbonates and these intermediates are acidic, it is hard for them to be adsorbed on the catalyst's
284 acidic surfaces. It is very easy for these formed intermediates to be desorbed from the surfaces of
285 the catalyst and this facilitates the positive improvement of the oxidation reaction of toluene (Hou
286 et al. 2019). For mesoporous materials like MCM-48, KIT-6, and SBA-15, pore size distribution
287 is narrow with high specific surface area, and Pd aggregation was found to be at a low rate

288 compared to other supports (Bendahou et al. 2008; Wang et al. 2008). The preparation method can
289 also affect the dispersion of Pd on its support. Various preparation techniques such as impregnation
290 and grafting techniques were investigated in order to understand the impact of the preparation
291 method on Pd dispersion during the synthesis of Pd supported on SBA-15. The grafting technique
292 was found to help in the formation of well-dispersed Pd particles on SBA-15 (He et al. 2010). The
293 solvent utilized in the synthesis was also found to exhibit a significant effect on the dispersion of
294 Pd. To understand the impact of various solvents on Pd dispersion on its support different solvents
295 like N,N-dimethylformamide, water, dimethyl sulphoxide, ethanol, and tetrahydrofuran were
296 investigated and the highest dispersion was shown on the catalyst synthesized by the use of N,N-
297 dimethylformamide (He et al. 2010). Another synthesis approach was reported to use two solvents
298 where they combine hydrophilic solvent like water and hydrophobic solvent like hexane. By using
299 this technique, SBA-15 supported Pd catalyst was prepared and the acid sites on the catalyst
300 showed advantages to the dispersion of Pd. Besides, the prepared catalyst was found to possess
301 good thermal stability and excellent tolerance to moisture. Of the tested catalyst prepared in this
302 way, the best one was observed to convert toluene totally at 210 °C with GHSV of 32,000 h⁻¹ (He
303 et al. 2012b).

304 Compared to the activity of Pd catalysts having a single type of pores on the support, Silica
305 materials bearing two different kinds of pores, such as micro- and mesopores were found to favor
306 the highest activity of the Pd catalyst when used as support. For instance, total toluene conversion
307 was achieved at 200 °C when silica material holding up both meso- and micropores was used as
308 support of the Pd catalyst. That reaction temperature was lower than that of catalysts having a
309 single type of pores (He et al. 2012c). Okumura et al. 2003 studied how Pd catalysts' catalytic
310 activity can be affected by the acid-base property of metal oxide support and found that the
311 electronic interaction between supports and Pd particles had an outstanding effect on the catalytic
312 performance of the catalyst.

313 The highest performance of Pd supported on bimodal mesoporous silica for toluene degradation
314 was investigated and Pd/BMS-15 was found to exhibit high catalytic activity towards toluene
315 oxidation compared to Pd/MCM-48 and Pd/MCM-41 catalysts. Besides, the prepared catalyst
316 (Pd/BMS-15) also showed improvement in hydrothermal stability at high GHSV (70,000 h⁻¹) for
317 1000ppm of toluene concentration (Qiao et al. 2015). The support effect over Pd supported

318 catalysts for toluene oxidation was studied where three different supports, including SiO₂, γ-Al₂O₃,
319 and TiO₂ were used for the investigation of the effect of support on the performance and properties
320 of Pd supported catalyst. The investigation was conducted for 1000ppm of toluene concentration
321 and 28,000 h⁻¹ of GHSV. The results showed the following order in catalytic performance:
322 1wt%Pd/TiO₂ > 1wt%Pd/SiO₂ > 1wt%Pd/γ-Al₂O₃ corresponds to T₉₀ = 208°C < T₉₀ = 224°C < T₉₀
323 = 240°C. The size of particles and the concentration of palladium on the surface of the support
324 were found to be affected by the strong interaction of support and palladium. The Pd/TiO₂
325 catalyst's excellent activity was attributed to the large size of the particles and the highest
326 concentration of palladium on the surface of the support (Kim et al. 2016).

327 The importance of basic sites with mechanistic studies of Pd-based catalyst supported on
328 modified-Al₂O₃ towards complete oxidation of toluene was studied. In that study, three different
329 metal oxides of Ba, Zr, and Mg were used for modifying Al₂O₃ support for Pd catalysts under the
330 reaction conditions of 500ppm toluene and 24,000 mL/g.h of GHSV. The results showed that the
331 Pd/Al₂O₃ performance was catalytically promoted in the following order: Pd/MgO-Al₂O₃ >
332 Pd/BaO-Al₂O₃ > Pd/ZrO₂-Al₂O₃ > Pd/Al₂O₃. The highest catalytic activity (T₅₀ = 185°C and T₉₀
333 = 209°C) of Pd/MgO-Al₂O₃ was due to PdO dispersion caused by its decrease in size (from 4.3
334 nm to 2.2 nm) observed after doping with MgO, which makes much Pd²⁺ to be present in the
335 catalyst (Weng et al. 2019). The preparation technique effect on the activity and surface features
336 of the OMS-2 supported Pd catalysts was also investigated where three different preparation
337 methods including deposition-precipitation (DP), pre-incorporation (PI), and ion-exchanging (EX)
338 were used to prepare Pd/OMS-2-DP, Pd/OMS-2-PI, and Pd/OMS-2-EX respectively with the same
339 metal loading of 0.5wt%, and the results showed that Pd/OMS-2-DP indicated excellent catalytic
340 performance compared to others where T₅₀ = 240°C and T₉₀ = 285°C. The highest catalytic activity
341 was due to the highest acidity, Pd loading surface, concentration of adsorbed oxygen, and higher
342 oxygen mobility (Liu et al. 2017). Zhao and Dong (2018) used SiH₄ to increase the stability of
343 Pd/Al₂O₃ in the aqueous oxidation reaction of toluene. In their work, they successfully prepared
344 Si-Pd/Al₂O₃ catalysts using SiH₄ treatment, and the stability of prepared catalysts were
345 significantly improved. From the reviewed literature, it can be noted that there are few reports
346 about the impact of active phase's oxidation state on the catalytic performance. Thus, further
347 studies can focus on the regulation of oxidation state of catalysts to develop more active Pd
348 catalysts for low-temperature toluene oxidation.

349 2.1.4 Silver-based catalysts

350 Like other noble metals, Ag-based catalysts have been used for oxidizing toluene. From the
351 reported literature, there are few reports about silver catalysts towards toluene oxidation. However,
352 Ag-based catalysts perform well for catalytic oxidation of toluene where it can achieve toluene
353 conversion of 93% at a low reaction temperature of 62 °C (Zhu et al. 2018b). Silver catalysts
354 supported on modified ceria for toluene removal at 40,000 h⁻¹ of GHSV and 1000ppm of toluene
355 concentration were investigated. It was observed that the silver-based catalyst supported on Mn₂O₃
356 with 0 to 2.1 of Ag loading range, 0.06 wt% Ag/Mn₂O₃ showed high activity yet poor stability for
357 the oxidation of toluene; however, after the addition of CeO₂, the catalyst exhibited very good
358 catalytic stability which was due to timely refilling of the surface reactive lattice oxygen molecules
359 (Zhang et al. 2019b). This shows that the addition of transition metal oxide to supported Ag catalyst
360 could influence the performance of the catalyst for this reaction.

361 Qin et al. 2017 used three different conditions for pretreatment such as O₂ at 500 °C, H₂ at
362 500 °C, and O₂ at 500 °C followed by H₂ at 300 °C to study their effect on the catalytic performance
363 of SBA-15 supported silver catalysts (Ag/SBA-15) for the oxidation of 1000ppm toluene over
364 GHSV of 37500 h⁻¹. Their results showed that big Ag particles were formed at the surface of the
365 support by the pretreatment under H₂ at 500 °C. After the pretreatment for O₂ at 500 °C, both Ag₂O
366 and Ag were formed, but the treatment of H₂ at 300 °C followed by pretreatment under O₂ at
367 500 °C leads to Ag₂O reduction and re-dispersion of Ag, resulting in the formation of smaller
368 particles of Ag. Thus, it can be concluded that various pretreatment conditions could highly affect
369 silver-based catalysts' structure, which in turn affects their adsorption capacity and catalytic
370 performance for toluene combustion. The effects of support

371 Table 1. Single noble metal-based catalysts for toluene oxidation

Catalysts	Supports	Metal loading (wt%)	Catalyst amount	Toluene concentration	GHSV (mL/g · h)	Temperature (°C)	Conversion (%)	Reference
Pt	CeO ₂	0.2	200 mg	1000ppm	48,000	150	90	(Peng et al.2016)
Pt	KBeta-SDS	1.1	100 mg	1000ppm	60 000	150	98	(Chen et al.2015)
Pt	CeO ₂ NW@SiO ₂	2	30 mg	1000ppm	20,000	167	90	(Peng et al.2019)
Pt	CeO ₂ /SiO ₂	2	30 mg	1000ppm	20,000	177	90	(Peng et al. 2019)
Pt	SiO ₂	2	30 mg	1000ppm	20,000	193	90	(Peng et al. 2019)
Pt	ZnO/SiC	0.03	50 mg	300ppm	20,000	210	100	(Li et al. 2017)
Pt	Ce/BEA	1	0.1g	22ppm	60,000	90	>99	(Xiao et al. 2018)
Pt	BEA	1	0.1g	22ppm	60,000	90	85	(Xiao et al. 2018)
Pt	CeO ₂	0.8	100 mg	200ppm	60,000	205	100	(Chen et al.2018)
Pt	3DOM CeO ₂ -Al ₂ O ₃	0.27	50 mg	1000ppm	20,000	198	90	(Yang et al.2016)
Pt	Co ₃ O ₄ /3DOM Al ₂ O ₃	1.3	50 mg	1000ppm	20,000	160	90	(Yang et al.2016)
Pt	TiO ₂	2	20 mg	1000ppm	160,000	190	100	(Lu et al. 2019)
Pt	ZSM-5	1.9	50 mg	1000ppm	60,000	155	100	(Chen et al.2015)
Pt	TiNT	0.4	0.2 g	500ppm	30,000	185	>95	(Rui et al. 2017)
Pt	Ce-C	1	150 mg	1000ppm	60,000	180	100	(Abdelouahab-reddam et al. 2015)
Pt	Al ₂ O ₃	0.1	100 mg	1000ppm	24,000	180	100	(Gan et al. 2019)
Pt	Zr-HMS	0.6	0.3 g	500ppm	20,000	200	100	(Parsafard et al. 2018)
Pt	HMS	0.6	0.3	500ppm	20,000	200	83	(Parsafard et al. 2018)
Pt	CuMnC	0.023	100 mg	2000ppm	5,000	216	90	(Zhu et al. 2018a)
Au	Fe ₂ O ₃ /GAC	0.2	0.2 g	630ppm	8,000	75	80	(Thanh et al. 2018)
Au	CeO ₂ /GAC	0.2	0.2 g	630ppm	8,000	75	80	(Thanh et al. 2018)
Au	MnO ₂	1.87	50 mg	1000ppm	60,000	205	90	(Sun et al. 2019a)

Au	MFS	1	70 mg	1000ppm	10,000	374	100	(Benais-Hamidi et al. 2015)
Au	CuO	1	50 mg	226ppmV	60,000	315	100	(Carabineiro et al. 2015)
Au	Fe ₂ O ₃	1	50 mg	226ppmV	60,000	345	100	(Carabineiro et al. 2015)
Au	La ₂ O ₃	1	50 mg	226ppmV	60,000	400	100	(Carabineiro et al. 2015)
Au	MgO	1	50 mg	226ppmV	60,000	387	100	(Carabineiro et al. 2015)
Au	NiO	1	50 mg	226ppmV	60,000	320	100	(Carabineiro et al. 2015)
Au	DOM Al ₂ O ₃	0.74	50 mg	1000ppm	20,000	317	90	(Yang et al. 2016a)
Au	3DOM CeO ₂ -Al ₂ O ₃	0.75	50 mg	1000ppm	20,000	279	90	(Yang et al. 2016b)
Au	Mn ₂ O ₃ /3DOM LSMO	5.92	50 mg	1000ppm	20,000	220	90	(Jiang et al. 2015)
Au	Mn ₂ O ₃ /3DOM SiO ₂	0.93	50 mg	1000 ppm	20,000	255	90	(Yang et al. 2015a)
Au	bulk Al ₂ O ₃	0.72	50 mg	1000ppm	20,000	360	90	(Yang et al. 2016a)
Pd	3DOM CeO ₂ -Al ₂ O ₃	0.29	50 mg	1000ppm	20,000	228	90	(Yang et al. 2016b)
Pd	BMS-15	0.41	50 mg	1000ppm	42,000	228	90	(Qiao et al. 2015)
Pd	OMS	0.5	50 mg	2000ppm	240,000	285	90	(Fu et al. 2017)
Pd	OMS-2-DP	0.5	50 mg	2000ppm	60,000	285	90	(Liu et al. 2017)
Ag	MnO ₂ -cordierite	2	0.05 g	1000ppm	10,000	275	90	(Zhu et al. 2019b)
Ag	Mn ₂ O ₃	0.06	50 mg	1000ppm	40,000	205	90	(Zhang et al. 2019d)
Ag	SBA-15	16	0.1 g	1000ppm	60,000	267	90	(Qin et al. 2017)
Ag	CeO ₂ /Al ₂ O ₃	1	0.05 g	600ppm	24,000	62	93	(Zhu et al. 2018b)
Ag	3DOM CeO ₂ -Al ₂ O ₃	0.81	50 mg	1000ppm	20,000	338	90	(Yang et al. 2016a)

373 structures on the interaction between OMS-2 support and Ag and the catalytic activity were
374 investigated, and the results revealed that the loaded Ag exercised crucial influence on catalyst
375 physicochemical properties, and the catalytic activity was highly improved (Fu et al. 2018). It
376 should be noted that few works on Ag-based catalysts for toluene oxidation were reported; thus
377 further research on their application for toluene oxidation is required.

378 **2.2 Noble metal alloy-based catalysts**

379 It has been found that supported noble metals alloy performs well for toluene oxidation compared
380 to supported single noble metals. Thus, some kinds of literature show that the catalytic
381 performance of noble metal-based catalysts could be furtherly increased by the addition of a second
382 noble metal (Fu et al. 2016). Au–Pd/3DOM Co₃O₄ for catalytic oxidation of toluene was studied.
383 In that study, gold-palladium alloy with a mass ratio of Au:Pd = 1:1 was supported on 3DOM
384 Co₃O₄ to make nanocatalysts, which achieved better performance than the supported single metals
385 (Pd or Au) catalyst. Of the tested catalysts, 1.99wt% AuPd/3DOM Co₃O₄ showed excellent
386 performance for catalytic toluene degradation where the temperatures to achieve 10%, 50%, and
387 90% conversion of toluene were 145, 164, and 168 °C at 40,000 mL•g⁻¹•h⁻¹ of space velocity,
388 respectively. In comparison with supported single metal (Au or Pd) catalyst, the prepared
389 nanocatalysts of 3DOM Co₃O₄ supported with Au–Pd showed good catalytic stability and higher
390 tolerance of moisture for the oxidation of toluene. Besides, the apparent activation energies of
391 xAuPd/3DOM Co₃O₄ (33–41 kJ mol⁻¹) was encountered to be less than the one of single Au or Pd
392 supported on 3DOM Co₃O₄ (52–112 kJ/mol), and it was concluded that the highest activity of
393 1.99wt% AuPd/3DOM Co₃O₄ was related to the ability of oxygen activation and strong interaction
394 of the noble metal with 3DOM Co₃O₄ (Xie et al. 2015a).

395 Pt-Pd bimetallic synthesis immobilized on MCM-41 mesoporous materials (Pt-Pd/MCM-41)
396 with super catalytic activity for toluene degradation was also investigated. The results revealed
397 that the prepared Pt-Pd/MCM-41 catalyst exhibited higher catalytic performance in comparison
398 with single Pt metal immobilized on MCM-41 (Pt/MCM-41) or Pd supported on MCM-41
399 (Pd/MCM-41) with the same amount of the metal of 0.3wt%. The total oxidation of toluene was
400 reached at 180 °C for 0.2Pt-0.1Pd/MCM-41 under 10,000 h⁻¹ of GHSV and 500ppm toluene. It
401 was also shown that the bimetal catalyst held large surface content of Pt (0) and a small size of

402 doped metal owing to the synergistic effect between the two noble metals, which resulted in
403 reducibility improvement and high capacity of adsorbing oxygen (Fu et al. 2016).

404 From Table 2, it is easily seen that the combination of gold (Au) and palladium (Pd) supported
405 on different supports is the one that is mostly used for toluene oxidation. Meanwhile, some of the
406 noble metals can be combined with other metals to increase their catalytic activity. For instance,
407 the combination of Au-Co supported on SBA-15 for catalytic degradation of toluene was
408 investigated and it was found that the prepared catalyst exhibited good catalytic activity for toluene
409 combustion where total degradation of toluene was reached at the reaction temperature of 300 °C.
410 It indicated that mesoporous materials provide extensive surface area support, and gold particles
411 get active supports from cobalt. Such a bimetallic catalyst helps overcome the deficiency of
412 specific surface area for reducible transition metal oxides (Wu et al. 2015). Similarly, Pt
413 immobilized on highly-dispersed ceria and activated carbon for complete VOCs degradation was
414 also investigated and platinum was promoted by ceria and high dispersion was achieved on
415 activated carbon as support. The prepared catalyst showed better performance for toluene
416 oxidation compared to platinum supported on bulk ceria due to the optimum synergistic energy
417 between high dispersion of ceria with particles of platinum (Abdelouahab-reddam et al. 2015). The
418 higher performance of platinum-supported catalysts could be attributed to the better Pt dispersion
419 on supports (Rui et al. 2017).

420 Hou et al. 2019 studied the tungsten effect for enhancing the catalytic activity of monolith
421 Pt/Ce_{0.65}Zr_{0.35}O₂ catalysts for toluene decomposition. Their study found a decrease of 30 °C in the
422 temperature for complete combustion of toluene using the monolith Pt-WO₃/Ce_{0.65}Zr_{0.35}O₂ catalyst
423 as compared to its counterpart without tungsten. The superior catalytic performance of Pt-
424 WO₃/Ce_{0.65}Zr_{0.35}O₂ was attributed to its excellent low-temperature reducibility, greater surface for
425 adsorbing high concentration of oxygen, and higher strength of the acidic medium.

426 Supports like silica materials were investigated to support bimetallic catalysts for deep
427 degradation of toluene (Fu et al. 2016). For example, SiO₂ supported Pd-Pt catalyst for toluene
428 combustion was studied and it was determined that during the reaction, the prepared catalyst
429 (0.25%Pd-0.25%Pt/SiO₂) had very limited coking and high activity for the reaction under reaction
430 conditions of 60,000 mL/g.h GHSV and 1000ppm toluene. That catalyst's performance

431 Table 2. Composite noble metal-based catalysts for toluene oxidation

Catalysts	Support	Metal Loading (wt%)	Catalyst amount	Toluene concentration	GHSV (mL/g.h)	Temperature (°C)	Conversion (%)	Reference
Pd-Pt	SiO ₂ -OA	0.25-0.25	100 mg	1000ppm	60,000	160	98	(Wang et al. 2017a)
Au-Pd	3DOM Co ₃ O ₄	1.99-1.99	50 mg	1000ppm	40,000	168	90	(Xie et al. 2015a)
Au-Co	SBA-15	2-15	100 mg	1100ppm	30,000	300	100	(Wu et al. 2015)
Au-Pd	Co ₃ O ₄	0.96-1.84	50 mg	1000ppm	40,000	180	90	(Wang et al. 2017b)
Au-Pd	Ce _{0.6} Zr _{0.3} Y _{0.1} O ₂	0.9-1.8	0.05 g	1000ppm	20,000	218	90	(Tan et al. 2015)
Au-Pd	3DOM Mn ₂ O ₃	3.8-7.3	50 mg	1000ppm	40,000	162	90	(Xie et al. 2015b)
Au-Ir	TiO ₂	2-2	100 mg	1000ppm	27,000	250	100	(Torrentemurciano et al. 2017)
Au-Pd	3DOM meso-Cr ₂ O ₃	1.95-3.9	50 mg	1000ppm	20,000	165	90	(Wu et al. 2016)
Pt-Pd	MCM-41	0.2-0.1	100 mg	500ppm	10,000	180	100	(Fu et al. 2016)
Pd-Au	NbTi	1-1	100 mg	1000ppm	60,000	200	15	(Barakat et al. 2018)
Pd-Au	VTi	1-1	100 mg	1000ppm	60,000	212	15	(Barakat et al. 2018)
Pt-WO ₃	Ce _{0.65} Zr _{0.35} O ₂	1-1	100 mg	1000ppm	12,000	220	100	(Hou et al. 2019)

432

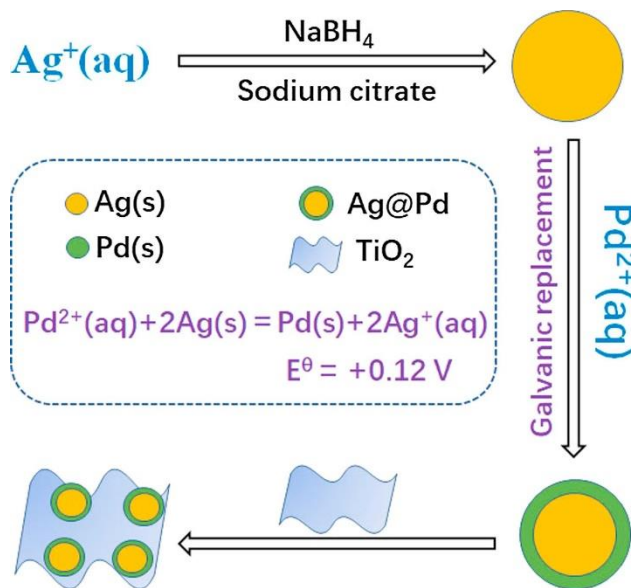
433 was determined to be ameliorated by the addition of oleic acid to the solution of metal salt during
434 the preparation of the catalyst, which was associated with the enhancement of Pd metal in the
435 formed catalyst (Wang et al. 2017a).

436 The recent industrial application needs catalysts with outstanding catalytic performance,
437 economy, and simple to design. Nowadays, it is still a pressing challenge to synthesize such
438 catalysts. It seems that the fabrication of a catalyst based on the co-doping of noble metals and
439 transition metals can be a solution owing to the high activity of noble metals, and the availability
440 and low cost of transition metals. Thus, it is recommended to explore the noble metals' fusion with
441 transition metals to develop cost-effective catalysts operational at low temperatures as it is noted
442 that no much research has been done on the combination of noble metals and transition metals.
443 Further work can focus on the effect of the second metal on the creation of active surface oxygen
444 of the catalyst. Other work can focus on dominant metals that can provide the maximum active
445 sites during the catalyst preparation based on the combination of noble and transition metals. A
446 deep study on the structure-activity relationship and synergistic effect of noble-transition metal
447 catalyst is also needed as it can be more beneficial for clearing some doubt like how various
448 structures and morphologies get formed which may result in different catalytic activities.

449 **2.3 Core-shell structured catalysts**

450 As stated earlier, noble metal-based catalysts have been commercially widely utilized in catalytic
451 oxidation of toluene due to their highest activity compared to other metals. However, they are
452 limited by their high cost and high metal load (Aboukaïs et al. 2016; Yang, Deng et al. 2016; Zhao
453 et al. 2019a). To increase their catalytic performance with lower metal loading, various techniques
454 to reduce the metal size in the nanometer scale like nanoparticles resulted in improving the active
455 surface areas, and mixing of noble metals with non-noble metals (Wu et al. 2015; Torrente-
456 murciano et al. 2017) or other noble metals (Xie et al. 2015b; Fu et al. 2016; Barakat et al. 2018)
457 have also attracted serious research attention. Core-shell structured catalysts have shown to be one
458 of the promising techniques to increase the catalyst activity and diminish its cost. Particularly,
459 core-shell structured catalysts based on two metals, like Ag@Pd and Au@ Pd, can optimize the
460 use of Pd metal in the shell and help in the cost reduction of the catalyst. It can also help catalytic
461 activity improvement through electronic alteration and reduced metal segregation of bimetallic
462 structures (Chen et al. 2016; Abdel-Fattah et al. 2017; Kang et al. 2018).

463 Bimetallic core-shell based catalysts have exhibited high catalytic performance towards toluene
 464 oxidation with lower metal loading. For instance, TiO₂ supported the core-shell structure of Ag
 465 and Pd bimetallic based catalyst for toluene oxidation was reported, and it was found that the
 466 prepared catalyst of Ag@Pd/TiO₂ exhibited higher catalytic activity for toluene oxidation in
 467 comparison with monometallic Pd/TiO₂ catalyst with Pd loading 25% wt (Li et al. 2018). Figure
 468 2 shows the preparation technique of Ag@Pd supported on TiO₂.



469
 470 Figure 2. Schematic representation of TiO₂ substrate supported Ag@Pd NPs core-shell structure
 471 synthesis (reproduced with permission from ref. (Li et al. 2018)).

472 Today, studies on Ag@M (M=Pt, Pd, Ru) core-shell catalysts have been conducted for oxygen
 473 reduction reaction (ORR) in fuel cell cathodes and production of hydrogen from the decomposition
 474 of formic acid (Wang et al. 2015). However, the reports about the utilization of those catalysts in
 475 the oxidation of toluene are still very few. Thus, more research about their activity on toluene
 476 oxidation might be worthy of being explored.

477 3. Transition metal-based catalysts

478 Current studies are focusing on the innovation of cheap catalysts with high catalytic performance
 479 at low temperatures. Generally, transition metals are less expensive as compared to noble metals.
 480 They are also abundant in nature and more resistant to poisons, but they usually have lower
 481 catalytic activity as compared to noble metal-based catalysts (Du et al. 2018; Feng et al 2018). The

482 most useful and effective transition metals for toluene oxidation are Mn, Co, and Ce, and other
483 metals like Fe, Cu, Ni, and Cr are not as effective as Mn, Co and Ce based on the experimental
484 results. Transition metals can be used as single metal-based catalysts with or without support (Li
485 et al. 2016a; Rokici et al. 2016; Wei et al. 2017; Xie et al. 2018; Ren et al. 2019; Zhu et al. 2019a).
486 The supported transition metal-based catalysts have been shown to have higher catalytic activity
487 compared to unsupported catalysts (Li et al. 2016). To increase the catalytic activity of transition
488 metal-based catalysts, two (Georgescu and Bombos 2016; Du et al. 2018; Jiang and Xu 2019;
489 Zhang et al. 2019c) or three (Dou et al. 2019) transition metals can be mixed to make one catalyst
490 with high performance. Tables 3 and 4 summarize reported single and mixed transition metal-
491 based catalysts, respectively. From Table 3, it is easily seen that Mn and Co-based catalysts are
492 mostly used as single metal-based catalysts for catalytic oxidation of toluene. Table 4 shows that
493 Mn is mostly mixed with other metals to make the bimetallic or trimetallic-based catalysts. Up to
494 now, the catalytic activity of single transition metal-based catalysts is still low compared to noble
495 metal-based catalysts; however, mixed transition metal-based catalysts can achieve comparable
496 catalytic performance to noble metal-based catalysts.

497 **3.1 Single transition metal-based catalysts**

498 As described earlier, transition metals can be used as single metal-based catalysts and have been
499 shown to perform well for catalytic oxidation of toluene (Wook et al. 2016; Qin et al. 2018). The
500 performance of single transition metal can depend on the shape of a catalyst as it affects the
501 catalyst's physicochemical properties. For instance, Ren et al. 2019 synthesized three different
502 shapes (1D, 2D, and 3D) of Co_3O_4 catalyst for toluene oxidation, and they found that the
503 performance of those three different shapes of the same catalyst was not the same, where 3D-
504 Co_3O_4 showed higher catalytic performance compared to others. The support nature can also affect
505 the performance of transition metal catalysts. For example, Chlala et al. 2016 prepared MnO_2
506 catalyst supported on two different supports (hydroxyapatite and Al_2O_3) and their results showed
507 that the catalyst supported on hydroxyapatite performed better than the one supported on Al_2O_3 .
508 The preparation method of a transition metal-based catalyst can be another factor affecting its
509 catalytic performance (Lin et al. 2018). It can also be affected by transition metal concentration on
510 the support (Rokici et al. 2017) as well as the morphology of the catalysts (Ren et al. 2018).

511 3.2 Mixed transition metal-based catalysts for toluene oxidation

512 It has been reported that mixed metal oxide catalysts exhibit better catalytic performance compared
513 to single metal oxides. For example, two different single oxides (CeO_2 , Co_3O_4) were combined to
514 study their synergistic effect on catalytic oxidation of toluene, and it was found that $\text{CeO}_2\text{-CoO}_x$
515 exhibited outstanding catalytic activity compared to pure CeO_2 and Co_3O_4 (Zhang et al. 2019d).
516 Dou et al. (2019) used environmentally friendly bacterial cellulose to synthesize $\text{CuO-CeO}_2\text{-ZrO}_2$
517 catalyst by a modified sol-gel method. The prepared catalyst exhibited excellent stability and
518 catalytic activity towards toluene oxidation where the total toluene conversion was reached at
519 220°C for 1500ppm toluene and $24,000\text{ h}^{-1}$ of GHSV. Their highest activity was ascribed to the
520 presence of many oxygen vacancies, a strong synergistic effect between metal-oxides, and
521 hierarchical porous structure.

522 A modified hydrothermal method was used to synthesize Mn-Ce oxide catalysts for low-
523 temperature toluene degradation and it was shown that the manganese-cerium ratio played an
524 essential role in catalysts preparation, textual properties, and catalytic performance. The creation
525 of Mn-Ce solid solution distinctly increases the surface area and pore volume of the catalyst.
526 Meanwhile, it has been found that Ce in Mn-Ce oxide played a key function in toluene adsorption,
527 but Mn was found to be important in toluene oxidation; hence the synergy of Mn and Ce
528 ameliorates the process of the catalytic reaction (Du et al. 2018).

529 The activity of mixed metal oxide catalysts could depend on the preparation method (Genty et
530 al. 2015) and the concentration of one of the mixed metals. Different Ce_aMnO_x catalysts were
531 synthesized for investigating the Ce concentration effect on the catalyst performance towards
532 toluene oxidation under $20,000\text{ mL/g} \cdot \text{h}$ of GHSV and 1000ppm of toluene. The results showed
533 that the performance order was $\text{Ce}_{0.03}\text{MnO}_x > \text{Ce}_{0.02}\text{MnO}_x > \text{Ce}_{0.04}\text{MnO}_x > \text{Ce}_{0.05}\text{MnO}_x > \text{MnO}_x$.
534 Among the tested catalysts, $\text{Ce}_{0.03}\text{MnO}_x$ showed the highest performance ($T_{50} = 215^\circ\text{C}$ and $T_{90} =$
535 225°C which are lower than those of MnO_x), stability, and high resistance to H_2O owing to
536 abundant oxygen molecules on the surface and species of Mn^{4+} (Zhao et al. 2019b).

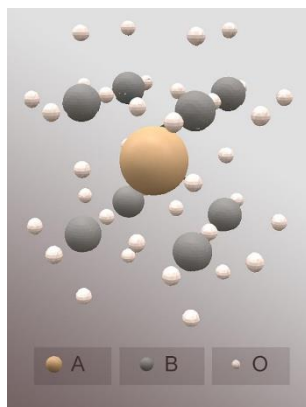
537 Table 3. Reported single transition metal-based catalysts for toluene oxidation

Catalyst	Support	Preparation method	Catalyst amount	Toluene concentration	GHSV (mL/g.h)	Temperature (°C)	Conversion (%)	Reference
MnO ₂	-	Template-free method	0.05 g	2000ppm	120,000	256	90	(Wei et al. 2017)
MnO ₂	Natural diatomite	Wet impregnation	3 g	200ppm	8,600	380	90	(Reza et al. 2016)
MnO ₂	Hydroxyapatite	Wet impregnation	0.2 g	800ppmv	30,000	220	100	(Chlala et al. 2016)
Ordered Mesoporous γ -MnO ₂	-	meso-Mn ₂ O ₃ +HNO ₃	50 mg	1000ppm	40,000	219	90	(Zeng et al. 2019)
MnO ₂ and Mn ₂ O ₃	Diatomite	Deposition-precipitation	200 mg	1000ppm	30,000	294	90	(Liu et al. 2017)
Mn ₃ O ₄	HACNFs	Thermal treatment	0.1 g	125ppm	11,250	280	99 ± 0.5	(Kang and Hwang 2020)
Mn ₃ O ₄	-	Hydrothermal	50 mg	200ppmv	6,000	150	100	(García et al. 2019)
MnO _x	-	Alkali-promoted redox precipitation	0.4 g	1000ppm	15,000	230	90	(Wang et al. 2016a)
MnO _x	MCM-41	Deposition	0.1 g	110ppm	30,000	Room temperature	99.4	(Yao et al. 2018)
MnO _x	Rod-like SBA-15	Precipitation	0.2 g	500ppm	15,000	230	>90	(Qin et al. 2018)
MnO _x	HZSM-5	Incipient impregnation	0.4 g	1000ppm	15,000	285	90	(Huang et al. 2016)
3D-Co ₃ O ₄ nanoflower	-	Template-free hydrothermal	100 mg	1000ppm	48,000	238	90	(Ren et al. 2019)
2D-Co ₃ O ₄ nanoplate	-	Template-free hydrothermal	100 mg	1000ppm	48,000	249	90	(Ren et al. 2019)

1D-Co ₃ O ₄ nanoneedle	-	Template-free hydrothermal	100 mg	1000ppm	48,000	257	90	(Ren et al. 2019)
Co	Sr-CeO ₂	Impregnation	0.45 g	1000ppm	20,000	330	100	(Feng et al. 2018)
Co	OMS-2	one step method	0.1 g	1000ppm	30,000	225	90	(Lin et al. 2018)
Co ₃ O ₄	-	Hydrogel-assisted route	0.1 g	1000ppm	60,000	297	90	(Rokici et al. 2016)
Co ₃ O ₄	3D nickel foam	Hydrothermal	0.145	1000ppm	41,000	270	100	(Zhang et al. 2018)
3D-Co ₃ O ₄	-	Hydrothermal	100 mg	1000ppm	48,000	248	90	(Ren et al. 2018)
FeO _x	-	Mild routes	100 mg	1000ppm	300,000	325	100	(Sanchis et al. 2018)
Fe ₂ O ₃	Al ₂ O ₃	Deposition	2 g	160ppm	15000	350	100	(Hee et al. 2017)
Cu	CeO ₂ -Nb ₂ O ₅	Wetness impregnation	150 mg	1000ppm	40,000	300	100	(Jardim et al. 2015)
CeO ₂	-	hydrothermal-driven assembly	100 mg	1000ppm	60,000	210	90	(Hu et al. 2018)
CeO ₂	-	Hydrothermal	0.05 g	0.8 ppm	27,600	350	100	(Duplančić et al. 2017)
Mesoporous NiO	-	Thermal decomposition reaction of Ni(NO ₃) ₂ · 9H ₂ O	0.1 g	500ppm	20,000	242	90	(Xia et al. 2017)

539 4. Perovskites catalysts

540 Perovskite catalysts belong to non-noble metal-based catalysts with ABO_3 as a formula in general,
541 where A represents rare earth or alkaline earth ion, B represents transition metal ions (Figure 1).
542 Other metal ions with similar radius can partly replace A and B so that their crystal structure
543 remains unchanged (Zang et al. 2019).



544
545 Figure 1. ABO_3 -type perovskite molecular model (reproduced with permission from ref. (Zang et
546 al. 2019)).

547 Perovskites based catalysts have been found to achieve excellent catalytic performance
548 similar to noble metal-based catalysts, but their very low surface area limits their practical
549 applications in catalytic combustion. Both intrinsic elements like surface area, surface oxygen
550 imperfection, A/B site, crystal structure, and extrinsic conditions such as preparation techniques
551 are known to significantly affect the catalytic activity of perovskite oxides type of catalysts. The
552 preparation methods are known to be correlated with the low surface area, especially for the
553 long-time reaction at high temperatures (Tomatis et al. 2016). Thus, it has been reported that the
554 increase of their surface area can be achieved by improving the preparation methods, decreasing
555 synthesis temperature, and applying supports of a high surface area (Li et al. 2009; Tomatis et al.
556 2016).

557 Table 4. Survey on reported mixed metal oxide catalysts for toluene oxidation

Catalyst	Support	Preparation method	Catalyst amount	Toluene concentration	GHSV (mL/g.h)	Temperature (°C)	Conversion (%)	Reference
CuCe _{0.75} Zr _{0.25} O _y	-	Sol-gel method	0.8 g	1500ppm	24,000	220	100	(Dou et al. 2019)
Co ₆ Al ₂ HTMW500	-	Microwaves	100 mg	1000ppm	60,000	273	100	(Genty et al. 2015)
Co ₆ Al ₂ HTUS500	-	Ultrasound	100 mg	1000ppm	60,000	280	100	(Genty et al. 2015)
Co ₆ Al ₂ HTCT500	-	Co-precipitation	100 mg	1000ppm	60,000	289	100	(Genty et al. 2015)
CoCr ₂ O ₄	γ-Al ₂ O ₃	Impregnation	0.11 g	700ppm	20,000	340	100	(Georgescu and Bombos 2016)
CeO ₂ -CoO _x	-	Co-precipitation	100 mg	500ppm	60,000	258	90	(Zhang et al. 2019d)
Cu-Mn	-	One-step hydrothermal	50 mg	1000ppm	10,000	169	90	(Luo et al. 2019)
Cu-O-Mn	γ-Al ₂ O ₃	Impregnation	50 mg	1000ppm	120,000	300	100	(Wang et al. 2017b)
Mn-Fe oxides	-	Reduction of KMnO ₄ by H ₂ O ₂ and hydrolysis of Fe salts	0.2 g	1000ppm	20,000	215	100	(Chen et al. 2017)
Co _{1.5} Mn _{1.5} O ₄	Ni foam	Hydrothermal	0.24 g	1000ppm	12,000	270	100	(Jiang and Xu 2019)
0.05La-Co	-	Co-precipitation		1000ppm	20,000	225	100	(Wu et al. 2019a)
10Fe-15Mn	γ-Al ₂ O ₃	Wet-impregnation	400 mg	1000ppm	3000	300	95	(Qin et al. 2019)
CuMn/La-4 mol%	-	Co-precipitation	55 mg	1000ppm	30,000	255	90	(Pan et al. 2019)
Mn _{0.6} Ce _{0.4} O ₂	-	Combination of redox-precipitation	0.2 g	500ppm	22500	210	100	(Du et al. 2018)

Cu-Mn-Ce	Cordierite honeycomb	and hydrothermal Incipient wetness	50 mg	100ppm	900	200	98	(Bo and Sun 2019)
Mn _{0.5} Ce _{0.5}	-	Simple precipitation	100 mg	1000ppm	60,000	245	90	(Wenxiang et al. 2015)
CuO-MnO _x	-	Precipitation	300 mg	600ppm	19,800	230	100	(Wei et al. 2019)
CuCe _{0.75} Zr _{0.25}	TiO ₂	Incipient impregnation	200 mg	500ppm	30,000	34	90	(Zhao et al. 2019a)
Cu _{0.5} Mn _{0.5} Ce _{0.75} Zr _{0.25}	TiO ₂	Incipient impregnation	200 mg	500ppm	30,000	38	90	(Zhao et al. 2019a)
MnCe _{0.75} Zr _{0.25}	TiO ₂	Incipient impregnation	200 mg	500ppm	30,000	84	90	(Zhao et al. 2019a)
Cu-Co	Halloysite	Wet-impregnation	0.2 g	600ppm	120,000	300	100	(Carrillo and Carriazo 2015)
Mn _{0.3} Zr _{0.7} O ₂	-	Partially substituting Zr ⁴⁺ in a ZrO ₂ with low-valent (Mn ²⁺)	200 mg	1000ppm	60,000	235	90	(Yang et al. 2018a)
Co ₆ Al _{2-y} Ce _y HT	-	Co-precipitation	100 mg	1000ppm	60,000	252	100	(Genty et al. 2016)
Ce _{0.03} MnO _x	-	Redox co-precipitation	0.3	1000ppm	20,000	220	90	(Zhao et al. 2019b)
Ce _{0.04} MnO _x	-	Redox co-precipitation	0.3	1000ppm	20,000	225	90	(Zhao et al. 2019b)
Ce _{0.05} MnO _x	-	Redox co-precipitation	0.3	1000ppm	20,000	230	90	(Zhao et al. 2019b)
Ce _{0.02} MnO _x	-	Redox co-precipitation	0.3	1000ppm	20,000	235	90	(Zhao et al. 2019b)

559 The effect of synthesis method on the catalytic performance of perovskite-type catalysts
560 towards toluene oxidation was studied through synthesizing highly active SmMnO₃ Perovskites
561 by using four different preparation methods, including impregnation, sol-gel, co-precipitation, and
562 self-molten-polymerization techniques (Liu et al. 2019a). The experimental results showed that
563 the perovskite synthesized by the self-molten-polymerization method exhibited the best catalytic
564 capacity compared to others. The highest catalytic activity of that catalyst could be ascribed to its
565 high concentration of adsorbed oxygen species, high surface ratio of Mn⁴⁺/Mn³⁺ (0.95) and lower
566 temperature reducibility. That catalyst showed long-term stability towards toluene oxidation by
567 maintaining the conversion of toluene >99.9% at 270 °C for 42 hours. Its oxidation reaction
568 depended on the synergistic effect between adsorbed oxygen, lattice oxygen, and oxygen vacancies.
569 The in-situ DRIFTS results indicated that the lattice oxygen on the surface of catalyst could
570 undergo electron transfers and form adsorbed oxygen species due to the activation by oxygen
571 vacancies (Liu et al. 2019a).

572 Meng et al. 2016 selected La_{n+1}Ni_nO_{3n+1} layered type of perovskite as a powerful catalyst for
573 toluene degradation to study the behavior of active oxygen species involved in the catalytic activity.
574 Their results demonstrated the order in toluene catalytic degradation of LaNiO₃ > La₄Ni₃O₁₀ >
575 La₂NiO₄ with 90% conversion of toluene at 250, 310, and 350 °C, respectively. This shows the
576 impact of transition metal parts on perovskite catalytic performance.

577 The effect of some metals on perovskite-type oxides' catalytic activity with a formula of
578 LaMn_{1-x}B_xO₃ (B=Cu, Fe and x=0, 0.3, 0.7), and La_{0.8}A_{0.2}Mn_{0.3}B_{0.7}O₃ (A=Sr, Ce and B=Cu, Fe)
579 was investigated and the experimental results revealed that Fe-based perovskite-type of catalysts
580 showed better catalytic performance than Cu-based perovskite-type of catalysts when subjected to
581 1000ppm with GHSV of 6000 h⁻¹. The replacement of Sr and Ce in the A-site place of the catalysts
582 increased their catalytic activity for toluene oxidation, and the highest activity was shown by
583 La_{0.8}Ce_{0.2}Mn_{0.3}Fe_{0.7}O₃ where T₅₀ and T₁₀₀ were 179 °C and 202 °C respectively (Tarjomannejad
584 et al. 2016). Sr²⁺ and Fe³⁺-doped LaMnO₃ perovskites catalysts (La_{0.9}Sr_{0.1}Mn_{0.9}Fe_{0.1}O₃) have been
585 synthesized, and that catalyst showed the highest performance comparable to many noble metal
586 catalysts in toluene catalytic oxidation, due to the presence of enriched surface oxygen vacancies
587 and mobile lattice oxygen (Weng et al. 2018).

588 The catalytic activity of perovskite-type catalysts can be increased by doping different transition
589 metals like Mn, Cu, and Fe (Meng et al. 2016; Suárez-vázquez et al. 2018). The performance of
590 perovskite catalyst can also depend on the treatment method; for example, Yang et al. (2018) found
591 that LaCoO_3 perovskite catalyst treated with acetic acid exhibited high catalytic performance
592 compared to untreated LaCO_3 where a decrease of 40 °C of the required temperature to convert
593 90% of toluene, was observed. It has been found that double-type perovskite catalysts exhibited
594 higher catalytic activity for toluene oxidation than single perovskite catalysts (Pan and Chang
595 2019).

596 The synthesis steps' effect on the catalytic performance of LaBO_3 (B: Mn, Fe) towards toluene
597 degradation was reported, where three successive synthesis steps, such as solid-state synthesis
598 (SSR), high-energy ball milling (HEBM), and low-energy ball milling (LEBM) in wet conditions,
599 were investigated. The results revealed that the catalytic performance for toluene oxidation rises
600 at each step, and the performance order was found to be $\text{SSR} < \text{HEBM} < \text{LEBM}$ (Heidinger et al.
601 2019). The supported perovskite catalysts were reported to exhibit higher catalytic performance
602 than the unsupported perovskite catalysts (Giroir-Fendler et al. 2016). Table 5 shows the summary
603 of perovskites-based catalysts reported on catalytic oxidation of toluene, and from this table, it can
604 be easily seen sol-gel method followed by calcination is the technique mostly used for the
605 preparation of perovskite-type catalysts.

606 The catalytic activity of perovskite can be tuned by changing its chemical composition because
607 it can hold metal elements of around 90% with no destruction of the structure. Furthermore, the
608 perovskite oxide's capacity for being stable at high temperatures enables them to be fitted for
609 thermal oxidation (Chen et al. 2019a). Therefore, more efforts can be put into the advancement of
610 perovskite catalysts with high performance, including control of morphology, dissolution
611 selectivity, replacement of A and/or B sites as well as the combination with precious metals.

612 Table 5. Reported perovskite-type catalysts for toluene oxidation

Catalyst	Preparation method	Catalyst amount	Toluene concentration	GHSV (mL/g.h)	Temperature (°C)	Conversion (%)	Reference
SmMnO ₃	One-step calcination	150 mg	1000ppm	24,000	240	99.9	(Liu et al. 2018)
LaNiO ₃	Coprecipitation + calcination	0.5 g	500ppm	19,200	250	90	(Meng et al. 2016)
La ₄ Ni ₃ O ₁₀	Coprecipitation + calcination	0.5 g	500ppm	19,200	310	90	(Meng et al. 2016)
La ₂ NiO ₄	Coprecipitation + calcination	0.5 g	500ppm	19,200	350	90	(Meng et al. 2016)
MnO ₂ /LaMnO ₃	One-step method	0.05 g	2000ppm	120,000	290	100	(Si et al. 2016)
LaMn _{0.3} Cu _{0.7} O ₃	Sol-gel auto combustion	0.2 g	1000ppm	60,000	220	100	(Tarjomannejad et al. 2016)
LaMn _{0.7} Fe _{0.3} O ₃	Sol-gel auto combustion	0.2 g	1000ppm	60,000	220	100	(Tarjomannejad et al. 2016)
LaMn _{0.3} Fe _{0.7} O ₃	Sol-gel auto combustion	0.2 g	1000ppm	60,000	215	100	(Tarjomannejad et al. 2016)
La _{0.8} Sr _{0.2} Mn _{0.3} Cu _{0.7} O ₃	Sol-gel auto combustion	0.2 g	1000ppm	60,000	215	100	(Tarjomannejad et al. 2016)
La _{0.8} Ce _{0.2} Mn _{0.3} Cu _{0.7} O ₃	Sol-gel auto combustion	0.2 g	1000ppm	60,000	210	100	(Tarjomannejad et al. 2016)
La _{0.8} Sr _{0.2} Mn _{0.3} Fe _{0.7} O ₃	Sol-gel auto combustion	0.2 g	1000ppm	60,000	205	100	(Tarjomannejad et al. 2016)
La _{0.8} Ce _{0.2} Mn _{0.3} Fe _{0.7} O ₃	Sol-gel auto combustion	0.2 g	1000ppm	60,000	202	100	(Tarjomannejad et al. 2016)
La _{0.9} Sr _{0.1} Mn _{0.9} Fe _{0.1} O ₃	SC-H ₂ O in a continuous hydrothermal flow reactor	0.3 g	500ppm	30,000	236	90	(Weng et al. 2018)
SrTi _{1-x} Mn _x O ₃	One pot hydrothermal	100 mg	1000ppm	60,000	335	90	(Suárez-vázquez et al. 2018)
SrTiO ₃	One pot hydrothermal	100 mg	1000ppm	60,000	354	90	(Suárez-vázquez et al. 2018)

$\text{SrTi}_{1-x}\text{Cu}_x\text{O}_3$	One pot hydrothermal	100 mg	1000ppm	60,000	398	90	(Suárez-vázquez et al. 2018)
$\text{LaMnO}_3/\delta\text{-MnO}_2$	Sol-gel	100 mg	1000ppm	30,000	275	100	(Yang et al. 2019a)
LaCoO_3	Citrate sol-gel	0.1 g	1000ppm	60,000	223	90	(Yang et al. 2018b)
$\text{La}_{1-x}\text{Sr}_x\text{MnO}_{3-\delta}$	One-step molten salt	500 mg	1000ppm	20,000	205	90	(Tian et al. 2016)
$\text{La}_2\text{CoMnO}_6$	Sol-gel-modified method	100 mg	300ppm	30,000	120	100	(Pan and Chang 2019)
LaMnO_3	One-step method under sc-H ₂ O	100 mg	500ppm	19,200	225	90	(Wang et al. 2016b)
$\text{LaMnO}_3/\text{TiO}_2$	Sol-gel	100 mg	1000ppm	60,000	303	90	(Giroir-Fendler et al. 2016)
$\text{LaMnO}_3/\text{YSZ}$	Sol-gel	100 mg	1000ppm	60,000	248	90	(Giroir-Fendler et al. 2016)

613

614 **5. MOFs-based catalysts**

615 Recently, metal-organic frameworks (MOFs) have shown prominently as versatile precursors that
616 can be applied to make functional MOF-derived materials for toluene catalytic oxidation. MOFs
617 composed of inorganic metal nodes and rigid organic linkers have captivated much attention to
618 make the metal oxides via the pyrolysis of organic linkers due to their adjustable, well-defined,
619 and highly porous structures (Peedikakkal et al. 2017; Luo et al. 2018; Chen et al. 2019b; Sun et
620 al. 2019c).

621 MOF-based catalysts have been reported to have an excellent catalytic performance for toluene
622 oxidation similar to noble metal-based catalysts where a single metal can be used to fabricate a
623 functional MOF-based catalyst (Zhao et al. 2019d), but mixed metal oxide can achieve higher
624 catalytic performance than a single one (Sun et al. 2019b).

625 MnO_x - CeO_2 -MOF and MnO_x -MOF as derived catalysts from MOFs were investigated. In that
626 study, MnO_x - CeO_2 -CP by co-precipitation and MnO_x -D by thermal decomposition of MnOOH
627 were synthesized for comparison and tested for 1000ppm toluene and 60,000 mL/g.h of GHSV.
628 The results showed that MOF-based catalysts (MnO_x - CeO_2 -MOF and MnO_x -MOF) exhibited
629 higher catalytic performance towards the oxidation of toluene compared to MnO_x - CeO_2 -CP and
630 MnO_x -D, and the order in catalytic performance was MnO_x - CeO_2 -MOF > MnO_x -MOF > MnO_x -
631 CeO_2 -CP > MnO_x -D (Sun et al. 2019b). The highest surface area and plentiful oxygen vacancies
632 resulted from the integration of Ce into MnO_x , and this resulted in excellent low-temperature
633 reducibility and high oxygen mobility, which would induce high content of Mn^{4+} on the surface
634 leading to the excellent activity of the catalyst (Sun et al. 2019b).

635 The $\text{MnO}_x/\text{Cr}_2\text{O}_3$ mixed metal catalyst by pyrolysis of MIL-101-Cr precursor for toluene
636 oxidation was investigated, and it was found that with the incorporation of MnO_x into Cr_2O_3 , the
637 $\text{MnO}_x/\text{Cr}_2\text{O}_3$ -MOF showed the obviously increased catalytic performance for the oxidation of
638 toluene in comparison with commercial Cr_2O_3 or pure Cr_2O_3 pyrolyzed by MIL-101-Cr (Chen et
639 al. 2019b). The as-prepared composite catalyst showed good stability, and the toluene conversion
640 could be remained at 85% for at least 240 hours without any catalyst deactivation. The better
641 durability and tolerance of the prepared catalyst were probably attributed to good stability for

642 crystal structure, oxygen vacancies, and reducibility (Chen et al. 2019b). Table 6 represents the
643 summary of the reported MOF-based catalysts for toluene oxidation and their synthesis methods.

644 Up to now, few articles have been reported on MOF-based catalysts, and only non-noble metal
645 catalysts derived from the metal-organic framework have been investigated; however, it is possible
646 to make noble metal-based catalysts derived from MOFs, and this can help to decrease the catalyst
647 cost, which will be more economical for industrial application.

648 **6. Spinel catalysts**

649 Spinel-based catalysts are metal oxides with a composition of AB_2O_4 and possess a defect-rich
650 structure (Tomatis et al. 2016). These catalysts have been reported to be less expensive and exhibit
651 high catalytic activity towards toluene oxidation at low temperatures (Wang et al. 2018). As the
652 synthesis method would affect the morphologies of the catalysts, it plays a crucial role in the
653 preparation of the spinel catalysts with higher surface area and required crystal structure (Tomatis
654 et al. 2016).

655 A template-free autoclave technique was used to synthesize a 3D flower-like morphology
656 $Co_{0.25}Mn_{0.75}O_4$ spinel catalyst. The as-prepared catalyst has been found stable and exhibits good
657 catalytic activity, and the total conversion of toluene was achieved at the reaction temperature of
658 239 °C, and no obvious change was found within 70 h of the reaction (Wang et al. 2018). The high
659 activity with the stability of the prepared spinel catalyst on toluene oxidation was associated with
660 its high surface area, porous structure, the interaction between Mn and Co, and rich surface oxygen
661 vacancies. In situ DRIFTS results showed the probable reaction pathway for synthetic Mn-Co
662 based catalyst, by which toluene was firstly dissociated to benzyl radical, benzaldehyde, benzene,
663 oxalic acid, and finally converted to CO_2 and H_2O (Wang et al. 2018).

664 Dong et al. (2019) synthesized nanoflower $CoMn_2O_4$ spinel catalyst using the oxalic acid sol-
665 gel method to investigate its performance in the catalytic toluene oxidation for GHSV of 22,500
666 mL/g.h and 500ppm of toluene concentration, and they found that compared to other metal oxides
667 like Co_3O_4 , MnO_x , and Co_3O_4/MnO_x , the synthesized spinel catalyst showed lower activation
668 energy of 35.5 kJ/mol, better catalytic performance (total conversion achieved at 220 °C), higher
669 surface area, richer cationic vacancy, and larger oxygen species mobility. The stability test showed

670 Table 6. Reported MOF-based catalysts for toluene oxidation

Catalyst	Preparation method	Catalyst amount	Toluene Concentration	GHSV (mL/g.h)	Temperature (°C)	Conversion (%)	Reference
Co ₃ O ₄ -ZIF-67	Pyrolysis of ZIF-67	0.6 g	12,000ppm	21,000	280	100	(Zhao et al. 2019c)
CeO ₂ -MOF	Pyrolysis of Ce-MOF precursor (Ce-(1,3,5-benze-netricarboxylic acid) (H ₂ O) ₆)	0.1 mg	1000ppm	20,000	223	90	(Chen et al. 2018)
Mn-Co-MOF	Pyrolysis of Mn-MOF (Mn ₃ [Co(CN) ₆] ₂ ·nH ₂ O)	0.05 g	500ppm	96,000	240 280	90 100	(Luo et al. 2018)
MnO _x /Cr ₂ O ₃ -MIL-101-Cr	Pyrolysis of MIL-101-Cr	0.1 g	1000ppm	20,000	270	90	(Chen et al. 2019b)
MnO _x -CeO ₂ -MOF-74	In situ pyrolysis of MOF-74	50 mg	1000ppm	60,000	210 220	50 90	(Sun et al. 2019b)
MnO _x -MOF-74	In situ pyrolysis of MOF-74	50 mg	1000ppm	60,000	227 230	50 90	(Sun et al. 2019b)

671

672 that the prepared spinel catalyst was very stable, and it was able to keep toluene conversion above
673 98% at 220 °C for about 700 min. Different types of oxygen species showed various roles in
674 catalytic oxidation of toluene. Therefore, in situ designed-temperature programmed (TP) methods
675 were used to study the participation of surface lattice oxygen, bulk lattice oxygen, and gaseous
676 oxygen in catalytic toluene oxidation over CoMn_2O_4 spinel catalysts. More specifically, the
677 gaseous oxygen moves to the bulk phase lattice and then migrates to the surface to form the surface
678 lattice oxygen on CoMn_2O_4 , the last of which deems to be the main active oxygen species in actual
679 toluene oxidation reaction (Dong et al. 2019).

680 A series of $\text{Mn}_{3-x}\text{Fe}_x\text{O}_4$ defected spinels were synthesized by controlling the integration of Fe
681 ions into the Mn_3O_4 crystal structure via self-polymerizable monomer adjustment of the molten
682 Mn-Fe salt dispersion. It was found that Fe doping raised the defected lattices, oxygen vacancy
683 concentration, specific surface area, mesoporosity, and catalytic properties compared to Cu ions
684 doping (Liu et al. 2019b). $\text{Mn}_{2.4}\text{Fe}_{0.6}\text{O}_4$ spinel catalyst showed the highest catalytic performance
685 for toluene oxidation where 90% conversion achieved at 224 °C for GHSV of 60,000 mL/g.h and
686 1000ppm toluene and no change have been found within 120 h, which confirms its stability (Liu
687 et al. 2019b).

688 In summary, from the reported literature, spinel catalysts showed good catalytic activity
689 towards toluene oxidation and, they have shown thermal stability and durability in the reported
690 experimental conditions; however, few types of research have been conducted on their application
691 in toluene catalytic degradation.

692 **7. Factors affecting the catalytic oxidation of toluene**

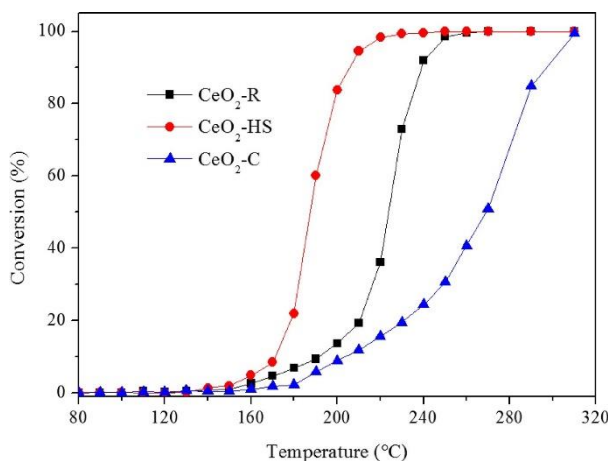
693 The success of catalytic oxidation of toluene is attributed to numerous factors that include the
694 reaction conditions and the activity of catalysts. The activity of the catalyst is mainly affected by
695 various factors, including morphology and structure, preparation techniques, degree of
696 crystallinity, surface reducibility, surface area, active components or sites, and stability (Zhang et
697 al. 2019e). The combination of these factors is desirable for a highly active catalyst to achieve
698 effective toluene degradation.

699 **7.1 Effects of morphology and structure**

700 The catalyst's morphology and structure play a crucial role in enhancing its catalytic performance.
701 The catalyst structure can affect other properties like surface area, pore size, and the available
702 active sites on the surface. The performance of manganese oxide catalysts with a square tunnel
703 structure has been mainly influenced by the size of tunnels (Molina et al. 2017). Similarly, the
704 active sites on the catalyst surface depend on the catalyst type. The shape effect of Pt/CeO₂ on the
705 toluene degradation was investigated where three different CeO₂ shapes such as nanoparticles,
706 nanorods, and nanocubes were used, and it was found that Pt/CeO₂-rods samples exhibited the
707 highest catalytic activity compared to others due to greatest reducibility and high oxygen vacancies
708 concentration on the surface. The experimental results showed that the performance of the
709 prepared catalysts depends on the morphology of the catalyst (Peng et al. 2016).

710 Similarly, The CeO₂ morphology effect on catalytic degradation of toluene was studied. In that
711 study, three different morphologies of CeO₂ catalysts (cube, hollow sphere (HS), and rod) were
712 prepared. The prepared catalysts were investigated for catalytic oxidation of toluene, and their
713 activities were compared. Of the tested catalysts, CeO₂-HS showed better catalytic performance
714 for toluene combustion compared to the rod and cube-shaped catalysts, which achieved 90% of
715 toluene conversion at 207 °C. Better performance of CeO₂-HS catalyst was ascribed to its high
716 surface area and large oxygen vacancies, which are essential for catalytic degradation of toluene.
717 Furthermore, CeO₂-HS showed good stability of the catalyst, reusability, and higher water
718 tolerance (Feng et al. 2019). As shown in Figure 3, the activity of CeO₂ catalysts depends on the
719 morphology of the catalyst.

720 The morphology effect of Ag/MnO₂ catalyst on catalytic degradation of toluene was also
721 investigated. In that study, three morphologies (wire-, rod- and tube-like) of Ag/MnO₂ catalyst
722 were prepared and tested for toluene oxidation. The experimental results showed that the tested
723 catalyst's catalytic performance depended on its morphology, and the wire-like Ag/MnO₂
724 exhibited higher catalytic activity towards toluene oxidation, which could achieve the complete
725 toluene degradation at 220 °C. The highest performance of this catalyst was attributable to the
726 strong interaction of Ag and MnO₂, which led to the high dispersion of hemispherical shape Ag
727 particles of small size, strong reducibility and formation of abundant active lattice oxygen (Li et
728 al. 2016).



729

730 Figure 3. Effect of CeO₂ morphologies (Rod, hollow sphere, and cube) on catalytic degradation
 731 of toluene (reproduced with permission from ref.(Feng et al. 2019)).

732 **7.2 Effect of preparation method and conditions**

733 Various methods of synthesizing catalysts, including precipitation, co-precipitation, facile sol-gel
 734 method (Peta et al. 2018), hydrothermal methods, and micro-emulsion processes (Zhang et al.
 735 2019f), are currently in use. Recently, researches have mostly focused on the improvement and
 736 modification of catalyst preparation techniques to increase their activity and catalytic performance
 737 (García et al. 2019; Peng et al. 2019; Wu et al. 2019b). Synthesis techniques and reaction
 738 conditions can be able to customize catalysts' textural properties, structures, and morphologies to
 739 influence their activity in oxidation reactions (He and Balasubramanian 2008; Okumura et al. 2003;
 740 Wang et al. 2008).

741 The grafting technique as one of the preparation methods used for preparing catalysts was found
 742 to help in the evolution of well-dispersed Pd particles on SBA-15 (He et al. 2010). The solvent
 743 utilized in the synthesis was also found to exhibit a significant influence on Pd's dispersion, where
 744 the highest dispersion was shown by the use of N,N-dimethylformamide (He et al. 2010). Other
 745 techniques for synthesis were reported to use an approach of two solvents where they combine
 746 hydrophilic solvent like water and hydrophobic solvent like hexane. Using this technique, the
 747 SBA-15 supported Pd catalyst was prepared, and the acid sites on the catalyst were determined to
 748 be related to Pd dispersion. Besides, the prepared catalyst was found to possess good thermal
 749 stability and excellent tolerance to moisture. Of the tested catalyst prepared in this way, the best

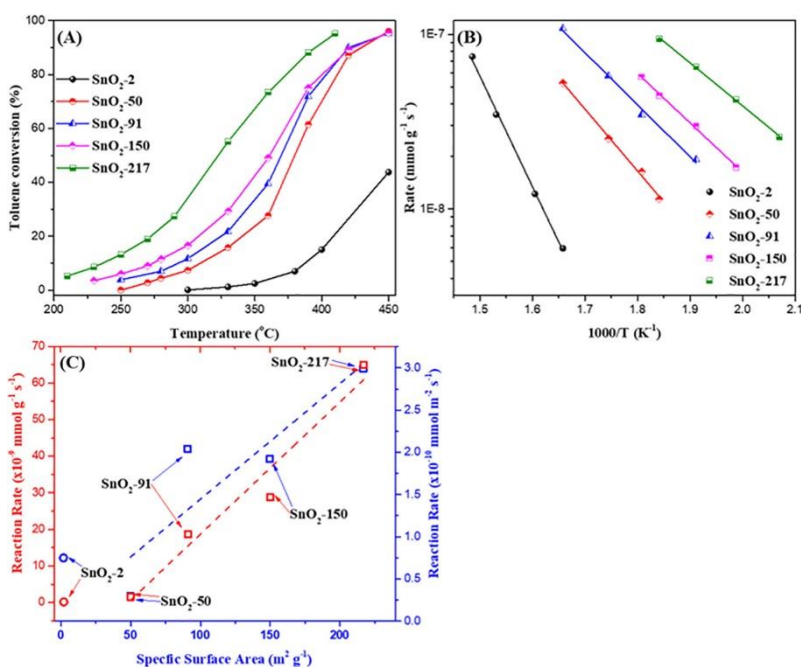
750 one was shown to convert toluene totally at 210 °C with GHSV of 32000 h⁻¹ (Yu et al. 2019; He
751 et al. 2012b).

752 MnO_x-CP by co-precipitation and MnO_x-D by thermal decomposition of MnOOH were
753 synthesized for comparison (Sun et al. 2019a). The experimental results showed that MnO_x-CP
754 exhibited higher catalytic activity towards toluene degradation as compared to MnO_x-D. The XPS
755 and H₂-TPR shows that the relative percentage of Mn⁴⁺ and low-temperature reducibility of
756 MnO_x-CP were higher than those of MnO_x-D, respectively. All these demonstrate that the
757 synthesis method might affect the interaction of MnO_x and support through electron transfer,
758 which would impact the catalytic activity of those catalysts. The influence of various synthesis
759 techniques on the textural properties of calcium tungstate (CaWO₄) and its catalytic properties in
760 the toluene degradation was investigated where CaWO₄ crystals were synthesized by microwave-
761 assisted hydrothermal (MAH) and polymeric precursor methods (PPM). The experimental results
762 showed that CaWO₄ synthesized by MAH, compared to CaWO₄ sample synthesized by PPM, have
763 higher oxygen mobility that appears to be a key factor for excellent catalytic activities (Alencar et
764 al. 2018).

765 **7.3 Effect of surface area**

766 The surface area of catalysts is an important morphological parameter affecting the catalytic
767 oxidation of toluene. Catalysts with a high surface area tend to exhibit better removal efficiencies.
768 Liu et al. 2018 investigated specific surface area impact on SnO₂ texture bulk and surface
769 properties with their effect on catalytic performance towards toluene degradation. Experimental
770 results demonstrated that a catalyst's textural properties such as pore volume and surface area
771 greatly affect its catalytic oxidation performance for toluene. It was shown that the adsorption
772 capacity and surface-active oxygen amount increase with the enhancement of the surface area,
773 which significantly increases the catalytic performance. To further study the effect of surface area,
774 five SnO₂ (SnO₂-2, SnO₂-50, SnO₂-91, SnO₂-150, and SnO₂-217) were prepared, for which the
775 last number shows the surface area of each in m²/g. From Figure 4A, it is shown that the
776 performance enhances in the following order: SnO₂-2 < SnO₂-50 < SnO₂-91 < SnO₂-150 < SnO₂-
777 217. This shows that the higher the surface area, the higher the catalyst activity, which implies that
778 the catalyst's surface area could play an important role in the reaction activity of toluene
779 combustion (Liu et al. 2018; Yusuf et al. 2020). To understand the surface area impact on inherent

780 performance, Arrhenius plots were collected, as shown in Figure 4B. From Figure 4C, it is
 781 observed that both R_s (reaction rate normalized by catalyst weight) and R_w (reaction rate
 782 normalized by catalyst surface area) improved with the increase of surface area. In addition, the
 783 impact of surface area on the catalyst activity was particularly discussed by Ren et al. (2018) for
 784 three-dimensional (3D) hierarchical Co_3O_4 nanocatalysts. The results demonstrated that the
 785 morphology-controlled 3D Co_3O_4 nanocatalysts (cube-stacked microspheres, plate-stacked
 786 flowers, needle-stacked double spheres and sheet-stacked fan-shaped catalysts) synthesized by
 787 various methods possessed quite different catalytic activities; and the cube-stacked microspheres
 788 showed the lowest T_{90} and best catalytic stability, attributable to its largest surface area, highly
 789 defective structure and exposure of $\{111\}$ crystal facet.



790
 791 Figure 4. Oxidation of toluene. (A) Toluene conversion, (B) Arrhenius plots, and (C) conversion
 792 rates (R_w and R_s) (reproduced with permission from ref. (Liu et al. 2018)).

793 7.4 Effect of relative humidity (RH)

794 The medium RH has a significant effect on the efficiency of toluene oxidation, but high RH
 795 influences water molecules to compete with toluene on the active sites of the catalyst. This
 796 diminishes the catalyst activity by blocking the active surface of the catalyst. Fang et al. (2009)
 797 reported a comparative study that the T_{90} under 90% RH increased by 6.4 - 15 % than the dry air

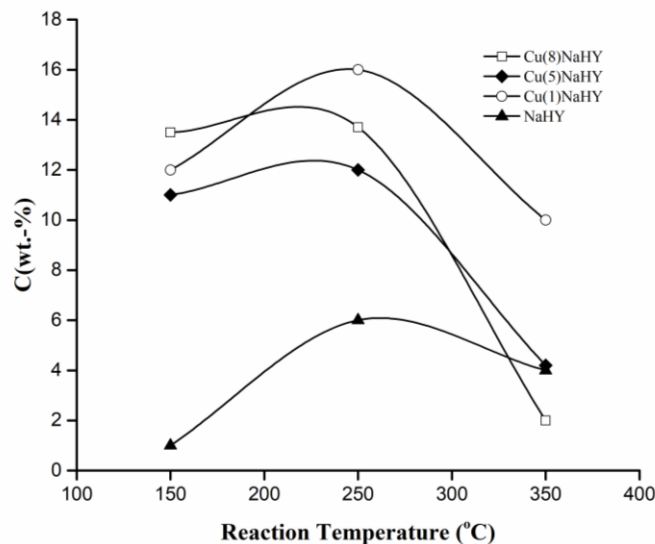
798 atmosphere for toluene degradation. Hydrophobic supports have been found to have the advantage
799 of avoiding the adsorption of moisture on the catalyst surface (Wu and Chang 1998). Thus, the
800 catalyst's active site could not be blocked, and the activity of the catalyst would be maintained.
801 Wu and Chang 1998 demonstrated that the higher hydrophobicity of the support, the lower the
802 temperature required for the complete conversion of toluene. To understand this, they prepared
803 three different catalysts with different hydrophobic supports and found out that the one with high
804 hydrophobicity showed the complete degradation of toluene at 150 °C while the other two with
805 less hydrophobicity achieved the completion oxidation at 180-200 °C. They also proposed that the
806 oxidation rate of toluene could be increased by the elimination of formed water from the reaction
807 system (Wu and Chang 1998). On the contrary, water vapor was found to help in the catalyst's
808 activity recovery by enabling the desorption of carbonates from the active surface of the catalyst
809 via the adsorption competition (Wang et al. 2015). Zhu and Andersson (1989) investigated the
810 effect of H₂O vapor on toluene oxidation over V₂O₅ and concluded that the addition of water of
811 the appropriate amount enhanced the catalyst performance for toluene oxidation and selectivity of
812 benzoic acid. Similarly, Ma et al. (2016) confirmed that toluene conversion and highest
813 benzaldehyde yield could be increased by H₂O added to the feed, and this phenomenon could be
814 attributed to the effect of H₂O adsorption on the catalyst surface that can behave as a hole trap
815 forming surface adsorbed hydroxyl radicals and suppress the electron-hole recombination so as to
816 enhance the catalytic oxidation of organic pollutants (Yusuf et al.2020). Different catalysts possess
817 various physiochemical properties and catalytic activities, hence it is worth of investigating how
818 the water vapor may promote the catalytic performance when designing the catalysts to be used.

819 **7.5 Formation of coke**

820 The formation of coke (carbon compounds) is frequently observed during the oxidation of VOCs.
821 These compounds were found to lower the catalyst activity and block the active catalyst site when
822 deposited on the pores and surface of the catalyst. The formation of coke and its removal for
823 catalytic oxidation of toluene on CuNaHY zeolites was investigated (Antunes et al. 2001). In this
824 study, the total burning of coke at 1020 °C using pyrolysis coupled with gas chromatography-mass
825 spectrometry (GC-MS) was applied to determine the amount and characterize the composition and
826 distribution of coke molecules deposited on the catalyst within 6 h after start of reaction. It was
827 observed that the percentage of deposited coke started to rise with reaction temperature (150-

828 250 °C) and then quickly decreased when the reaction temperature increased further as shown in
829 Figure 5. In this figure, the percentage of coke on NaHY was lower due to its much lower apparent
830 overall conversion efficiency than CuNaHY. The characterization analysis shows the coke on
831 NaHY mainly contained the aromatic hydrocarbons and oxygenated compounds, but the former
832 got converted to oxygenated compounds at 250°C, which was the insoluble coke appearing from
833 250°C upwards and becoming the major coke components at 350°C. However, the oxygenated
834 components were predominant on CuNaHY catalysts at 150°C and more oxygenated molecules
835 formed when copper content increased. These findings confirmed the role of copper in oxygen
836 activation that was promoting the oxidation of hydrocarbons. Different from NaHY, the quantity
837 of oxygenated compounds decreased when the temperature increased and the insoluble part of
838 coke reached a maximum at 250°C. Besides, only insoluble coke was observed at 350°C on
839 Cu(8)NaHY. Based on the distribution of coke molecules, the presence of copper leads to a high
840 performance in toluene oxidation and an improvement of the oxidation of coke components.

841 The temperature effect on the formation of coke was also described in the oxidation of *o*-xylene
842 over Pd/HY (Magnoux and Guisnet 1999). It was observed that when the reactant oxidation is very
843 fast, the formed coke becomes low. From the experimental observation, the amount of coke
844 retained on the catalyst might also depend on the acidity of the support as the presence of acidic
845 sites might influence the dispersion of active elements (Dégé et al. 2000). The formation of coke
846 was widely reported on zeolites, and various methods were specifically designed to quantify and
847 characterize coke formation on these materials (Beauchet et al. 2007; Pinard et al. 2013). Coke
848 formation could be avoided by enhancing the operating temperature above 290 °C, and the
849 deactivated catalysts could be regenerated by increasing the temperature to destroy the retained
850 coke (Magnoux and Guisnet 1999).



851

852 Figure 5. The percentage of carbon (C, wt%) deposited on NaHY and CuNaHY catalysts after 6
 853 hours reaction (reproduced with permission from ref. (Antunes et al. 2001)).

854 7.6 Effect of halogen poisoning

855 Halogen-containing compounds are utilized as essential precursors, agents for controlling the
 856 morphology (Tanada et al. 1999), and raw materials for making various catalysts, especially noble
 857 metal catalysts (Xu et al. 2015b). However, different noble metal catalysts such as Pt catalysts
 858 have been found to be deactivated by halogenated compounds like Cl and F containing compounds
 859 where these anions block Pt active sites (Gracia et al. 2002; Nie et al. 2014). As described in
 860 section 2, noble metal catalysts have shown good catalytic activity towards the oxidation of toluene,
 861 and Pt catalysts exhibit better catalytic performance than others. Nevertheless, Pt active sites in
 862 the catalysts are easily deactivated by halogens. Gracia et al. 2002 investigated the chlorine effect
 863 on Pt catalysts for oxidation reaction and revealed that the presence of chlorine seriously affected
 864 the catalyst activity where the catalyst with chlorine was ten times less active than the catalyst
 865 without chlorine. Nie et al. 2014 also showed that the adsorbed F⁻ ions on the Pt catalyst surface
 866 decrease the catalyst performance and may lead to total deactivation. Halogens such as F, Cl, Br,
 867 and I in halogen-containing VOCs deactivate the catalysts during their catalytic oxidation or when
 868 they are mixed with other VOCs like toluene (Deng et al. 2020; Lv et al. 2020).

869 Zhu et al. 2016 studied the effect of halogen poisoning on Pt-TiO₂. In their work, Pt catalysts
870 supported on TiO₂ were prepared with or without halogens like Cl⁻, F⁻, Br⁻ and I⁻ ions.
871 Experimental results showed that the activity of halogen-free catalysts was much higher than the
872 activity of halogen-containing catalysts. By comparing the catalytic activity of halogen-containing
873 catalysts, the results showed their activity in the following order: F-Pt > Cl-Pt > Br-Pt > I-Pt. The
874 strong halogen adsorption on the Pt nanoparticle surface was the cause of poisoning (Zhu et al.
875 2016). The mechanism for halogen poisoning showed that the coordination bonds are formed
876 between the adsorbed halogen ions and atoms of Pt by electron transfer into unoccupied 5d orbit
877 of Pt atom, then inhibiting the adsorption of oxygen and lead to the catalyst inactivation (Zhu et
878 al. 2016).

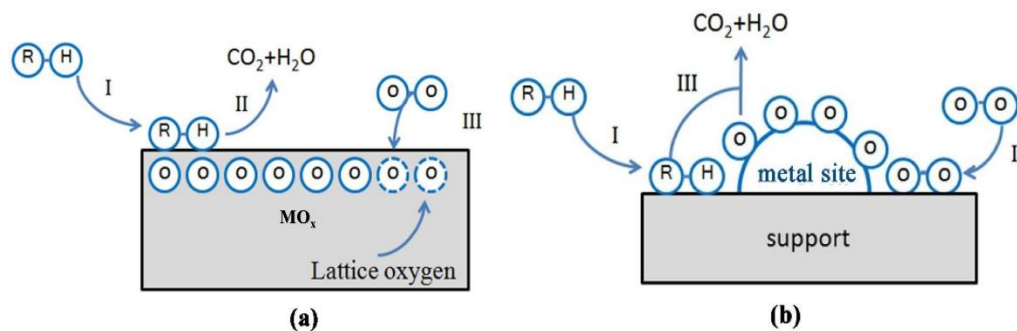
879 Halogen poisoning does not affect metal catalysts at the same level. For instance, Cao et al.
880 2018 studied the deactivation mechanism of Pd-, Pt- and Ru-TiO₂ catalysts for dichloromethane
881 oxidation. Their results showed that Pt/TiO₂ had lower performance and was easily get poisoned,
882 while Ru/TiO₂ showed high resistance for chlorine poisoning. Compared to noble metals catalysts,
883 transition metal catalysts are resistant to halogen poisoning (Yang et al. 2015b; Yang et al. 2019b).
884 The resistance of transition metal catalysts to poison may occur due to their higher active surface
885 area (Spivey 1987). Zhao et al. 2020 showed that zeolites such as ZSM-5 and BEA are resistant to
886 the adsorption of chlorine due to their large surface area. Huang et al. (2015) reported CeO₂-based
887 catalysts for Chloro-aromatics degradation and found that CeO₂ catalyst's stability was highly
888 dependent on the Deacon activity where species of chlorine could be eliminated as Cl₂.

889 **8. Reaction mechanisms and kinetics of toluene catalytic oxidation**

890 A kinetic model is an important tool for the simulation of toluene combustion/oxidation and the
891 evaluation of toluene degradation efficiency under different operational conditions. There are three
892 types of kinetic models for catalytic degradation of toluene: Power law (PL), Langmuir, and Mars–
893 van Krevelen (MVK) models. The Power-law model appears not to provide the description of
894 reaction chemistry and there is no direct connection to the mechanisms of reactions. Langmuir
895 model is built on E-R (Eley-Rideal) and L-H (Langmuir-Hinshelwood) mechanisms. E-R
896 mechanism supposes that the reaction occurs between the adsorbed oxygen and gaseous toluene
897 rather than the toluene which is adsorbed. The L-H mechanism supposes that the adsorbed oxygen
898 reacts with adsorbed toluene. MVK model describes the adsorbed toluene reacts first with oxygen

899 inside the catalyst and then the reduction of metal oxides takes place; after that, the reduced metal
900 oxides undergo reoxidation by gas phase oxygen. Based on the literature, the MVK model is more
901 widely used when it comes to the degradation of toluene by various metal-based catalysts (Lyu et
902 al. 2020).

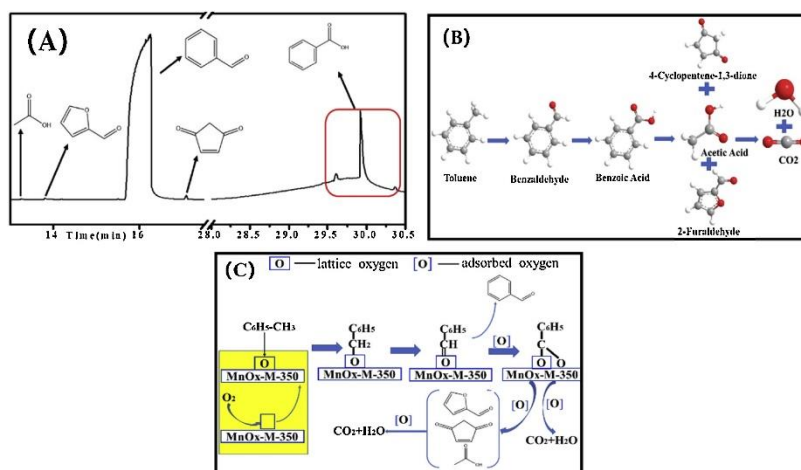
903 Understanding the reaction mechanism of catalytic oxidation of toluene by different types of
904 catalysts is one of the key points for developing a suitable catalyst of low cost, high performance,
905 and good stability. As mentioned earlier, there are different types of catalysts for toluene oxidation,
906 and those catalysts may have different reaction mechanisms due to their various structure and
907 composition that may influence different intermediate species formation. In general, the proposed
908 reaction mechanisms for catalytic toluene degradation fall into two major categories: Mars-van
909 Krevelen (MVK) model (major) and Langmuir-Hinshelwood (L-H) model (minor) (Kamal et al.
910 2016). In the MVK model (Figure 6a), which is also called the redox mechanism, the reaction
911 occurs between the adsorbed toluene and the catalyst's lattice oxygen instead of gaseous oxygen.
912 This model assumes that toluene oxidation occurs in two steps. In the initial step, the metal oxide
913 reduction results from the reaction between oxygen in a catalyst and adsorbed toluene, while in
914 the next step, there is a reoxidation of reduced metal oxide caused by gaseous oxygen available in
915 the feed (Zang et al. 2019).



916
917 Figure 6. Schematic of MVK (a) and L-H (b) mechanisms (reproduced with permission from ref.
918 (Yang et al. 2019b)).

919 In the Langmuir-Hinshelwood (L-H) model (Figure 6b), the reaction occurs at the catalyst
920 surface. The first step of this model is the adsorption of toluene and oxygen on the surface of the
921 catalyst, then the redox process takes place later. In this mechanism, the toluene adsorption and
922 catalyst's surface oxygen are necessary because the reaction occurs between these two types of

923 adsorbed molecules (Zang et al. 2019). Thus, different catalysts will have different reaction
 924 mechanisms and kinetics due to their compositions. Hosseini et al. 2012 reported that toluene
 925 oxidation reaction follows the L-H model when Pd-Au/TiO₂ is used as a catalyst. In this reaction,
 926 the toluene molecule has been found to compete with the oxygen molecule for getting adsorbed
 927 on the surface of the catalyst. The reaction mechanism and reaction pathway of toluene degradation
 928 over MnOx-M-350 catalyst was studied. During the study, XPS results of O1s showed that the
 929 majority of oxygen species on the catalyst's surface were lattice oxygen and adsorbed oxygen
 930 (Guo et al. 2019). Firstly, the reaction occurs at the catalyst's surface where the C–H bond of –CH₃
 931 from adsorbed toluene reacts with the lattice oxygen as stated by the MVK mechanism, resulting
 932 in benzaldehyde intermediates generation where their aldehyde groups are further oxidized to
 933 benzoic acid intermediates that will react with adsorbed oxygen to give CO₂ as shown in Figure 7.



934
 935 Figure 7. (A) TD/GC–MS results of the intermediates of toluene oxidation at 200 °C. (B) Pathway
 936 for catalytic degradation of toluene; (C) Reaction mechanism for the oxidation of toluene over
 937 MnOx-M-350 catalyst (reproduced with permission from ref. (Guo et al. 2019)).

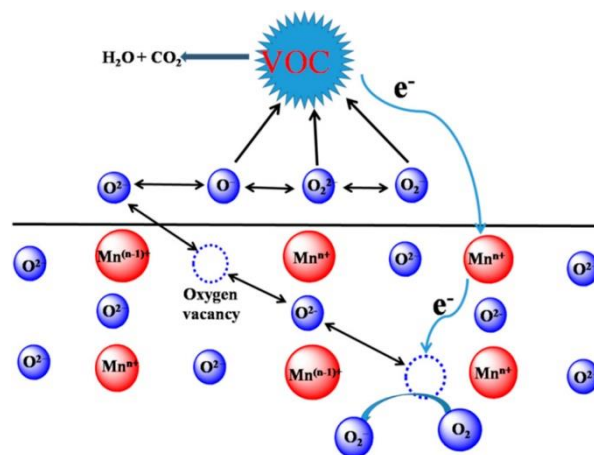
938 Dong et al. 2019 proposed the reaction mechanism of toluene oxidation catalyzed by a
 939 CoMn₂O₄ spinel catalyst. In the proposed mechanism, the first step is the oxidation of adsorbed
 940 toluene to alkoxide caused by surface oxygen, followed by the oxidation of alkoxide to benzoate,
 941 then benzoate is oxidized to anhydride that will be oxidized to acetate, and finally, acetate is
 942 oxidized to CO₂ as shown in Figure 8.



943

944 Figure 8. Proposed mechanism for toluene oxidation over CoMn_2O_4 spinel (reproduced with
 945 permission from ref. (Dong et al. 2019)).

946 Interestingly, Liu et al. (2019a) reported the change mechanism of active species ions during
 947 the toluene oxidation over SmMnO_3 perovskite catalyst. In their work, they used the in-situ
 948 DRIFTS method in N_2 to change the catalyst's surface structure by removing the adsorbed oxygen
 949 species on the catalyst surface. At 120 °C, no significant change was found in the infrared spectrum
 950 before the addition of toluene, but immediate infrared spectrum change was observed right after
 951 feeding toluene, showing that various reactions occurred on the catalyst surface. Although no
 952 oxygen was added to the system, characteristic peaks of CO_2 , $-\text{OH}$, $-\text{COOH}$, and $-\text{CO}_3^{2-}$ appeared
 953 in the spectrum, and their intensities increased with reaction temperature. This showed the
 954 involvement of lattice oxygen in the oxidation of toluene. From Figure 9, it can be easily seen that
 955 there is a formation of CO_2 and H_2O from the reaction between VOC molecules and adsorbed
 956 oxygen overflow from oxygen vacancies. The movement of lattice oxygen to the surface, the
 957 creation of adsorbed oxygen, and the change of Mn^{n+} to $\text{Mn}^{(n-1)+}$ by electron transfer were caused
 958 by the generation of oxygen vacancies. There was continuous adsorption of gas-phase oxygen into
 959 oxygen vacancies, and this facilitates the reduction of Mn^{n+} to $\text{Mn}^{(n-1)+}$ and acceptance of electrons
 960 from the reactants for the formation of molecular oxygen (O_2^-). The continuous appearance of
 961 VOC molecule oxidation was promoted by the conversion of molecular oxygen into lattice oxygen
 962 and active adsorbed oxygen (Liu et al. 2019b). For this case, it is the change mechanism of active
 963 species where the oxidation reaction was dependent on the synergism of lattice oxygen, adsorbed
 964 oxygen, and oxygen vacancies. Hence, the reaction mechanism shows a combination of MKV and
 965 L-H models.



966

967 Figure 9. The mechanism for migration and transformation of SmMnO₃ surface oxygen
 968 (reproduced with permission from ref. (Liu et al. 2019)).

969 Behar et al. (2015) used the above three models to study the kinetics of the oxidation of toluene
 970 over Cu_{1.5}Mn_{1.5}O₄ catalyst. It shows that only the results from MKV model can agree with
 971 experimental data and it was concluded that the reaction obeys the MVK mechanism. PL model
 972 was applied to study the kinetics of the degradation of toluene over 4 various manganese-based
 973 catalysts synthesized by different techniques. Experimental data were found to fit the modeling
 974 outcomes (Sihaib et al. 2017).

975 Niu et al. (2018) investigated the reaction kinetics of catalytic oxidation of toluene over Cu₁₋
 976 _yMn₂Ce_yO_x/sepiolite catalyst using two different kinetic models, including Power-rate Law and
 977 MVK models. Their results revealed that Power-rate Law was unsuitable for the description of the
 978 toluene oxidation reaction kinetic over the catalysts, but the MVK mechanism was found to be a
 979 good model for describing toluene catalytic degradation kinetics as it provided a better fit ($R^2 \geq$
 980 0.99) with the experimental data. MVK kinetic model was built up based on the redox process,
 981 including the oxidation and reduction steps. In the oxidation step, toluene gets adsorbed and reacts
 982 at the oxidation active sites, resulting in the formation of oxidation products and reduced active
 983 sites; in the reduction step, the oxygen gets reduced at the reduced active sites and then the
 984 oxidation state activity can occur (Niu et al. 2018). The kinetic model was expressed as: $-r_i =$
 985 $K_i C_i \theta$ and $-r_{oi} = K_{oi} C_{oi} (1 - \theta)$, where θ is coverage rate of the surface oxidation activity of the
 986 catalyst; $-r_i$ and $-r_{oi}$ are reaction rate of VOCs and oxygen consumption ($\text{mol} \cdot (\text{cm}^3 \cdot \text{s})^{-1}$),
 987 respectively; K_i and K_{oi} are the rate of catalyst surface reduction and oxidation reaction (s^{-1}),

988 respectively; and C_i and C_{oi} are the concentration of VOCs and oxygen ($\text{mol}\cdot(\text{cm}^3)^{-1}$), respectively.
989 1 mol VOCs were oxidized to consume α_i mol oxygen, and $-r_{oi} = -\alpha_i\cdot r_i$ could be calculated. Thus,
990 for this approach, measured rate of reaction (Eq.1) is expressed based on the above equations.

$$991 \quad \frac{1}{r_i} = \frac{\alpha_i}{K_{oi}C_{oi}} + \frac{1}{K_iC_i} \quad (\text{Eq.1})$$

992 The conversion of toluene to CO_2 is a complex process and multistep reaction. Shortly, step
993 one is the toluene adsorption on the surface of the catalyst via abstraction of H from methyl group
994 to generate benzoyl and later form aromatic ring-based intermediates like benzyl alcohol,
995 benzaldehyde, and benzoate molecules. Then, the aromatic rings on the intermediates are attacked
996 by the surface oxygen to form other intermediates without aromatic ring, like carboxylate and
997 maleic anhydride which will then undergo oxidation to form H_2O and CO_2 . The lattice oxygen
998 consumed for the whole process could be refilled by gas-phase oxygen. The properties of the
999 catalysts could determine the intermediates produced in the reaction. Investigating the kinetics and
1000 mechanism of catalytic reaction provides a deeper comprehension of catalytic reaction processes
1001 and an effective guidance for the enhancement of catalyst activity. From the literature, there are
1002 few reports on kinetics and reaction mechanisms of toluene catalytic oxidation over various types
1003 of catalysts. Therefore, it is needed for further studies on the mechanism and kinetics of toluene
1004 oxidation under different catalysts in a deep and comprehensive way. This will help researchers to
1005 get more information and a basis for designing cost-effective catalysts for industrial applications.
1006 Future research can also focus more on the combination of MKV and L-H models.

1007 **9. Conclusion and perspectives**

1008 In this review paper, we present a brief investigation of catalytic degradation of toluene over five
1009 different types of catalysts, including noble metal, transition metal, perovskite, metal-organic
1010 framework (MOFs), and spinel-based catalysts, and sum up the techniques improving their activity.
1011 Noble metal catalysts show excellent performance at low temperatures, even less than $100\text{ }^\circ\text{C}$, but
1012 in practical application, they are limited by their high cost and scarcity. Transition metals are
1013 plentiful and cheap compared to noble metals, but their based catalysts are restricted by their low
1014 performance. Recent studies have paid much attention to the amelioration and exploitation of
1015 different morphologies and structures of these transition metal catalysts. Thus, more studies are
1016 still needed in the amelioration of their structured morphologies and redox properties.

1017 Various factors like active metal elements, used support, specific surface area, dispersion of the
1018 active metal on the support, doping of other metal elements, particle size, and preparation methods
1019 could influence catalysts' catalytic activity towards toluene oxidation. The use of mixed/composite
1020 metal based on more than one noble metal or transition metal, which can be supported or
1021 unsupported, was also reported to enhance the performance of the catalyst. As challenges in the
1022 catalytic technology of toluene are still confusing, there is a need for innovations in the
1023 development of new catalysts that can be cheaper, more stable, selective, durable, and that can
1024 work at the lower reaction temperature. There are few research papers reported on metal-organic
1025 framework (MOFs), core-shell, and spinel-based catalysts for toluene oxidation, and those
1026 catalysts have been found to exhibit high catalytic performance at low temperatures. Therefore,
1027 future research should focus on the invention of non-noble metal-based catalysts derived from
1028 metal-organic frameworks to decrease the cost and reaction temperature for the total conversion
1029 of toluene.

1030 Furthermore, the doping of noble metals in the core-shell and spinel catalysts should be
1031 explored. Besides, as the synthesis methods are correlated to the specific surface area, preparation
1032 methods should be focused on enhancing the surface area of perovskite catalysts, and this should
1033 overcome their limitations of low surface area. Development of molecular modeling using
1034 theoretical calculations and models for predicting the reaction's behavior and simulating the effects
1035 of heat- and mass transfer in the system should also be exploited. For instance, quantitative
1036 structure-activity relationship research could be used to design the appropriate catalyst, simulating
1037 and developing models for designing reactors.

1038 **Ethics approval and consent to participate**

1039 Not applicable.

1040 **Consent for publication**

1041 Not applicable.

1042 **Authors contributions**

1043 David Murindababisha: Conceptualization, Writing-original draft. Yong Sun: Supervision,
1044 Writing-review & editing. Abubakar Yusuf: Conceptualization, Methodology, Formal analysis.

1045 Chengjun Wang: Resources, Funding acquisition, Writing-review & editing. Yong Ren:
1046 Methodology, Writing-review & editing. Jungang Lv: Resources, Conceptualization. Hang Xiao:
1047 Investigation, Writing-review & editing. George Zheng Chen: Supervision, Writing-review &
1048 editing. Jun He: Funding acquisition. Supervision, Writing-review & editing.

1049 **Competing interests**

1050 The authors declare that they have no competing interests.

1051 **Availability of data and materials**

1052 Data sharing is not applicable to this review article as no datasets were generated or analyzed
1053 during the current study.

1054 **Acknowledgments**

1055 The authors acknowledge the financial supports from Ningbo Science and Technology Innovation
1056 2025 Key Project (2020Z100), Start-up Research Funding of South-Central University of
1057 Nationalities (YZZ18018), and Provincial Key Laboratory Program by Zhejiang Provincial
1058 Department of Science and Technology (No. 2020E10018).

1059 **Acronyms**

1060 3DOM LSMO: Three-dimensionally ordered macroporous $\text{La}_{0.6}\text{Sr}_{0.4}\text{MnO}_3$

1061 3DOM: Three-dimensional Ordered Macroporous

1062 BMS: bimodal mesoporous silica

1063 Ce-C: Ceria on activated carbon

1064 GAC: Granular activated carbon

1065 GHSV: Gas hourly space velocity

1066 HACNFs: Hollow activated carbon nanofibers

1067 HT: Hydrotalcite

1068 KBeta-SDS: K^+ form of an aluminum-rich Beta zeolite- seed-directed synthesis

- 1069 MCM-41: Mobil Composition of Matter No. 41
- 1070 MOFs: Metal-Organic Frameworks
- 1071 NPs: Nanoparticles
- 1072 OA: Oleic Acid
- 1073 OMS: Octahedral molecular sieve
- 1074 OMS-2-DP: Octahedral molecular sieve-2-deposition precipitation
- 1075 SBA-15: Santa Barbara Amorphous-15
- 1076 SC-H₂O: Supercritical water
- 1077 TiNT: TiO₂ nanotube
- 1078 YSZ: Y₂O₃-ZrO₂
- 1079 ZIFs: Zeolitic imidazolate frameworks
- 1080 Zr-HMS: ZrO₂ modified hierarchical porous silica

1081 **References**

- 1082 Abdel-Fattah WI, Eid MM, Abd El-Moez SI, Mohamed E, Ali GW (2017) Synthesis of biogenic
1083 Ag@Pd Core-shell nanoparticles having anti-cancer/anti-microbial functions. *Life Sci* 183:28–36.
1084 <https://doi.org/10.1016/j.lfs.2017.06.017>
- 1085 Abdelouahab-Reddam Z, Mail R El, Coloma F, Sepúlveda-Escribano A (2015) Platinum
1086 supported on highly-dispersed ceria on activated carbon for the total oxidation of VOCs. *Appl*
1087 *Catal A, Gen* 494:87–94. <http://doi.org/10.1016/j.apcata.2015.01.026>
- 1088 Aboukais A, Skaf M, Hany S, Cousin R, Aouad S, Labaki M, Abi-Aad E (2016) A comparative
1089 study of Cu, Ag and Au doped CeO₂ in the total oxidation of volatile organic compounds (VOCs).
1090 *Mater Chem Phys* 177:570–576. <http://doi.org/10.1016/j.matchemphys.2016.04.072>
- 1091 An N, Li SY, Duchesne P, Wu P, Zhang W, Lee JF, Cheng S, Zhang P, Jia M, Zhang WX (2013)
1092 Size effect of platinum colloid particles on the structure and CO oxidation properties of supported
1093 Pt/Fe₂O₃ catalysts. *J Phys Chem C*. 117:21254–21262. <https://doi.org/10.1021/jp404266p>
- 1094 Alencar LDDS, Lima NA, Mesquita A, Probst LFD, Batalha DC, Rosmaninho MG, Fajardo HV,
1095 Balzer R, Bernardi MIB (2018) Effect of different synthesis methods on the textural properties of
1096 calcium tungstate (CaWO₄) and its catalytic properties in the toluene oxidation. *Mater Res* 21:
1097 e20170961. <https://doi.org/10.1590/1980-5373-mr-2017-0961>

- 1098 Antunes AP, Ribeiro MF, Silva JM, Ribeiro FR, Magnoux P, Guisnet M (2001) Catalytic oxidation
1099 of toluene over CuNaHY zeolites: Coke formation and removal. *Appl Catal B, Environ* 33:149–
1100 164. [https://doi.org/10.1016/S0926-3373\(01\)00174-6](https://doi.org/10.1016/S0926-3373(01)00174-6)
- 1101 Barakat T, Rooke JC, Chlala D, Cousin R, Lamonier J, Giraudon J, Casale S, Massiani P, Su B
1102 (2018) Oscillatory behavior of Pd-Au catalysts in toluene total oxidation. *catalysis* 8:574.
1103 <https://doi.org/10.3390/catal8120574>
- 1104 Beauchet R, Magnoux P, Mijoin J (2007) Catalytic oxidation of volatile organic compounds
1105 (VOCs) mixture (isopropanol/o-xylene) on zeolite catalysts. *Catal Today* 124:118–123.
1106 <https://doi.org/10.1016/j.cattod.2007.03.030>
- 1107 Behar S, Gómez-Mendoza NA, Gómez-García MÁ, Świerczyński D, Quignard F, Tanchoux N
1108 (2015) Study and modelling of kinetics of the oxidation of VOC catalyzed by nanosized Cu–Mn
1109 spinels prepared via an alginate route. *Appl Catal A* 504:203-210.
1110 <https://doi.org/10.1016/j.apcata.2014.12.021>
- 1111 Benais-Hamidi F, Chérif-Aouali L, Siffert S, Cousin R, Bengueddach A (2015) Total oxidation of
1112 toluene over gold supported on mesoporous ferrisilicates materials. *Int J Environ Pollut.* 58:187–
1113 196. <https://doi.org/10.1504/IJEP.2015.077177>
- 1114 Bendahou K, Cherif L, Sffert S, Tidahy H., Benaissa H, Aboukais A (2008) The effect of the use
1115 of lanthanum-doped mesoporous SBA-15 on the performance of Pt/SBA-15 and Pd/SBA-15
1116 catalysts for total oxidation of toluene. *Appl Catal A, Gen* 351:82–87.
1117 <https://doi.org/10.1016/j.apcata.2008.09.001>
- 1118 Bo L, Sun S (2019) Microwave-assisted catalytic oxidation of gaseous toluene with a Cu-Mn-
1119 Ce/cordierite honeycomb catalyst. *Front Chem Sci Eng* 13:385–392.
1120 <https://doi.org/10.1007/s11705-018-1738-3>
- 1121 Bravo H, Sosa R, Sánchez P, Bueno E, González L (2002) Concentrations of benzene and toluene
1122 in the atmosphere of the southwestern area at the Mexico City Metropolitan Zone. *Atmos Environ.*
1123 36:3843–3849. [https://doi.org/10.1016/S1352-2310\(02\)00292-3](https://doi.org/10.1016/S1352-2310(02)00292-3)
- 1124 Cao S, Fei X, Wen Y, Sun Z, Wang H (2018) Bimodal mesoporous TiO₂ supported Pt, Pd and Ru
1125 catalysts and their catalytic performance and deactivation mechanism for catalytic combustion of
1126 Dichloromethane (CH₂Cl₂). *Appl Catal A, Gen.* 550:20–27.
1127 <https://doi.org/10.1016/j.apcata.2017.10.006>
- 1128 Carabineiro SAC, Chen X, Martynyuk O, Bogdanchikova N, Avalos-borja M, Pestryakov A,
1129 Tavares PB, Órfão JJM, Pereira MFR, Figueiredo JL (2015) Gold supported on metal oxides for
1130 volatile organic compounds total oxidation. *Catal Today* 244:103–114.
1131 <http://dx.doi.org/10.1016/j.cattod.2014.06.034>
- 1132 Carrillo AM, Carriazo JG (2015) Cu and Co oxides supported on halloysite for the total oxidation
1133 of toluene. *Appl Catal B, Environ* 164:443–452. <http://dx.doi.org/10.1016/j.apcatb.2014.09.027>
- 1134 Chen B, Wang B, Sun Y, Wang X, Fu M, Wu J, Chen L, Tan Y, Ye D (2019) Plasma-Assisted
1135 Surface Interactions of Pt/CeO₂ catalyst for enhanced toluene catalytic oxidation. *Catalysts* 9: 2.
1136 <https://doi.org/10.3390/catal9010002>
- 1137 Chen C, Chen F, Zhang L, Pan S, Bian C, Zheng X, Meng X, Xiao FS (2015a) Importance of

- 1138 platinum particle size for complete oxidation of toluene over Pt/ZSM-5 catalysts. *Chem Commun*
1139 51:5936–5938. <https://doi.org/10.1039/C4CC09383F>
- 1140 Chen C, Wang X, Zhang J, Bian C, Pan S, Chen F, Meng X, Zheng X, Gao X, Xiao F (2015b)
1141 Superior performance in catalytic combustion of toluene over mesoporous ZSM-5 zeolite
1142 supported platinum catalyst. *Catal Today* 258:190–195.
1143 <https://doi.org/10.1016/j.cattod.2015.02.006>
- 1144 Chen C, Wang X, Zhang J, Pan S, Bian C, Wang L, Chen F, Meng X, Zheng X, Gao X, Xiao FS
1145 (2014) Superior performance in catalytic combustion of toluene over KZSM-5 zeolite supported
1146 platinum catalyst. *Catal Letters*. 144:1851–1859. <https://doi.org/10.1007/s10562-014-1295-4>
- 1147 Chen C, Zhu J, Chen F, Meng X, Zheng X, Gao X, Xiao F (2013) Enhanced performance in
1148 catalytic combustion of toluene over mesoporous Beta zeolite-supported platinum catalyst. *Appl*
1149 *Catal B Environ* 141:199–205. <https://doi.org/10.1016/j.apcatb.2013.03.050>
- 1150 Chen D, Li J, Cui P, Liu H, Yang J (2016) Gold-catalyzed formation of core-shell gold-palladium
1151 nanoparticles with palladium shells up to three atomic layers. *J Mater Chem A* 4:3813–3821.
1152 <https://doi.org/10.1039/C5TA10303G>
- 1153 Chen H, Wei G, Liang X, Liu P, He H, Xi Y (2019a) The distinct effects of substitution and
1154 deposition of Ag in perovskite LaCoO₃ on the thermally catalytic oxidation of toluene. *Appl Surf*
1155 *Sci* 489:905–912. <https://doi.org/10.1016/j.apsusc.2019.06.009>
- 1156 Chen J, Chen X, Xu W, Xu Z, Chen J, Jia H, Chen J (2017) Hydrolysis driving redox reaction to
1157 synthesize Mn-Fe binary oxides as highly active catalysts for the removal of toluene. *Chem Eng J*
1158 330:281–293. <https://doi.org/10.1016/j.cej.2017.07.147>
- 1159 Chen X, Cai S, Yu E, Jia H, Chen X, Chen X, Cai S, Yu E, Chen J, Jia H, et al (2019b) MnO_x/Cr₂O₃
1160 composites prepared by pyrolysis of Cr-MOF precursors containing in situ assembly of MnO_x as
1161 high stable catalyst for toluene oxidation. *Appl Surf Sci* 475:312–324.
1162 <https://doi.org/10.1016/j.apsusc.2018.12.277>
- 1163 Chen X, Yu E, Cai S, Yu E, Jia H, Cai S, Liang P, Chen J, Chen J (2018) In situ pyrolysis of Ce-
1164 MOF to prepare CeO₂ catalyst with obviously improved catalytic performance for toluene
1165 combustion. *Chem Eng J* 344:469–479. <https://doi.org/10.1016/j.cej.2018.03.091>
- 1166 Chlala D, Giraudon J, Nuns N, Lancelot C, Vannier R (2016) Active Mn species well dispersed
1167 on Ca²⁺ enriched apatite for total oxidation of toluene. *Appl Catal B Environ* 184:87–95.
1168 <https://doi.org/10.1016/j.apcatb.2015.11.020>
- 1169 Cui BC, Yi HH, Tang XL, Wang YE, Liu X, Li YT (2016) Status and progress of treatment
1170 technologies of toluene in industrial waste gas. *Mod Chem Ind* 36:30–33.
1171 <https://doi.org/10.16606/j.cnki.issn0253-4320.2016.02.008> (In Chinese)
- 1172 Debecker DP, Stoyanova M, Rodemerck U, Eloy P, Le A, Su B, Gaigneaux EM (2010) Thermal
1173 spreading as an alternative for the wet impregnation method: Advantages and downsides in the
1174 preparation of MoO₃/SiO₂-Al₂O₃ metathesis catalysts. *J Phys Chem C* 114:18664–18673.
1175 <https://doi.org/10.1021/jp1074994>
- 1176 Dégé P, Pinard L, Magnoux P, Guisnet M (2000) Catalytic oxidation of volatile organic
1177 compounds II. Influence of the physicochemical characteristics of Pd/HFAU catalysts on the

- 1178 oxidation of o-xylene. *Appl Catal B Environ* 27:17–26. <https://doi.org/10.1016/S0926->
1179 3373(00)00135-1
- 1180 Deng H, Pan T, Zhang Y, Wang L, Wu Q, Ma J (2020) Adsorptive removal of toluene and
1181 dichloromethane from humid exhaust on MFI, BEA and FAU zeolites: An experimental and
1182 theoretical study. *Chem Eng J* 394:124986. <https://doi.org/10.1016/j.cej.2020.124986>
- 1183 Dong C, Qu Z, Qin Y, Fu Q, Sun H, Duan X (2019) Revealing the highly catalytic performance
1184 of spinel CoMn_2O_4 for toluene oxidation: Involvement and replenishment of oxygen species using
1185 In Situ Designed-TP techniques. *ACS Catal.* 9:6698–6710.
1186 <https://doi.org/10.1021/acscatal.9b01324>
- 1187 Dou B, Zhao R, Yan N, Zhao C, Hao Q, Hui KS (2019) A facilitated synthesis of hierarchically
1188 porous Cu–Ce–Zr catalyst using bacterial cellulose for VOCs oxidation. *Mater Chem Phys*
1189 237:121852. <https://doi.org/10.1016/j.matchemphys.2019.121852>
- 1190 Du J, Qu Z, Dong C, Song L, Qin Y, Huang N (2018) Low-temperature abatement of toluene over
1191 Mn-Ce oxides catalysts synthesized by a modified hydrothermal approach. *Appl Surf Sci*
1192 433:1025–1035. <https://doi.org/10.1016/j.apsusc.2017.10.116>
- 1193 Duplančić M, Kurajica S, Tomašić V, Minga I (2017) Catalytic oxidation of toluene on
1194 hydrothermally prepared ceria nanocrystals. *Chem Biochem Eng Quart.* 31:375–383.
1195 <https://doi.org/10.15255/CABEQ.2017.1098>
- 1196 Ezeh CI, Tomatis M, Yang X, He J, Sun C (2018) Ultrasonic and hydrothermal mediated synthesis
1197 routes for functionalized Mg-Al LDH: Comparison study on surface morphology, basic site
1198 strength, cyclic sorption efficiency and effectiveness. *Ultrason. Sonochem.* 40: 341-352.
1199 <https://doi.org/10.1016/j.ultsonch.2017.07.013>
- 1200 Fang J, Chen X, Xia Q, Xi H, Li Z (2009) Effect of relative humidity on catalytic combustion of
1201 toluene over copper based catalysts with different supports. *Chinese J Chem Eng* 17:767–772.
1202 [http://dx.doi.org/10.1016/S1004-9541\(08\)60275-X](http://dx.doi.org/10.1016/S1004-9541(08)60275-X)
- 1203 Feng X, Guo J, Wen X, Xu M, Chu Y, Yuan S (2018) Enhancing performance of Co/CeO₂ catalyst
1204 by Sr doping for catalytic combustion of toluene. *Appl Surf Sci* 445:145–153.
1205 <https://doi.org/10.1016/j.apsusc.2018.03.070>
- 1206 Feng Z, Ren Q, Peng R, Mo S, Zhang M, Fu M (2019) Effect of CeO₂ morphologies on toluene
1207 catalytic combustion. *Catal Today* 332:177–182. <https://doi.org/10.1016/j.cattod.2018.06.039>
- 1208 Fu J, Dong N, Ye Q, Cheng S, Kang T, Dai H (2018) Enhanced performance of the OMS-2 catalyst
1209 by Ag loading for the oxidation of benzene, toluene, and formaldehyde. *New J Chem* 42:18117–
1210 18127. <https://doi.org/10.1039/C8NJ04030C>
- 1211 Fu X, Liu Y, Yao W, Wu Z (2016) One-step synthesis of bimetallic Pt-Pd/MCM-41 mesoporous
1212 materials with superior catalytic performance for toluene oxidation. *Catal Commun* 83:22–26.
1213 <https://doi.org/10.1016/j.catcom.2016.05.001>
- 1214 Fu Z, Liu L, Song Y, Ye Q, Cheng S, Kang T, Dai H (2017) Catalytic oxidation of carbon
1215 monoxide, toluene, and ethyl acetate over the xPd/OMS-2 catalysts: Effect of Pd loading. *Front*
1216 *Chem Sci Eng* 11:185–196. <https://doi.org/10.1007/s11705-017-1631-5>

- 1217 Gan T, Chu X, Qi H, Zhang W, Zou Y, Yan W, Liu G (2019) Pt/Al₂O₃ with ultralow Pt-loading
1218 catalyze toluene oxidation: Promotional synergistic effect of Pt nanoparticles and Al₂O₃ support.
1219 *Appl Catal B Environ* 257:117943. <https://doi.org/10.1016/j.apcatb.2019.117943>
- 1220 García T, Manuel J, Mayoral Á, Zhang Y, Arenal R, Alonso-domínguez D, Pilar M, Luisa M,
1221 Dejoz A, Icb-csic IDC, Luesma CM (2019) Green synthesis of cavity-containing manganese
1222 oxides with superior catalytic performance in toluene oxidation. *Appl Catal A, Gen* 582:117107.
1223 <https://doi.org/10.1016/j.apcata.2019.06.005>
- 1224 Genty E, Brunet J, Pequeux R, Capelle S, Siffert S, Cousin R (2016) Effect of Ce substituted
1225 hydrocalcite-derived mixed oxides on total catalytic oxidation of air pollutant . *Mater Today Proc*
1226 3:277–281. <http://dx.doi.org/10.1016/j.matpr.2016.01.069>
- 1227 Genty E, Brunet J, Poupin C, Casale S, Capelle S, Massiani P, Siffert S, Cousin R (2015) Co-Al
1228 mixed oxides prepared via LDH Route using microwaves or ultrasound: Application for catalytic
1229 toluene total oxidation. *Catalysts* 5:851–867. <https://doi.org/10.3390/catal5020851>
- 1230 Georgescu V, Bombos D (2016) Complete oxidation of toluene on Co-Cr mixed oxide catalyzt.
1231 *Rev Chim* 67:2258-2261. <https://doi.org/10.37358/Rev.Chim.1949>
- 1232 Giroir-Fendler A, Alves-Fortunato M, Richard M, Wang C, Díaz JA, Gil S, Zhang C, Can F, Bion
1233 N, Guo Y (2016) Synthesis of oxide supported LaMnO₃ perovskites to enhance yields in toluene
1234 combustion. *Appl Catal B Environ* 180:29–37. <https://doi.org/10.1016/j.apcatb.2015.06.005>
- 1235 Gracia FJ, Miller JT, Kropf AJ, Wolf EE (2002) Kinetics, FTIR, and controlled atmosphere
1236 EXAFS study of the effect of chlorine on Pt-supported catalysts during oxidation reactions. *J Catal*
1237 209:341–354. <https://doi.org/10.1006/jcat.2002.3601>
- 1238 Guo M, Li K, Liu L, Zhang H, Guo W, Hu X (2019) Manganese-based multi-oxide derived from
1239 spent ternary lithium-ions batteries as high-efficient catalyst for VOCs oxidation. *J Hazard Mater*
1240 380:120905. <https://doi.org/10.1016/j.jhazmat.2019.120905>
- 1241 Han L, Cai S, Gao M, Hasegawa JY, Wang P, Zhang J, Shi L, Zhang D. (2019) Selective catalytic
1242 reduction of NO_x with NH₃ by using novel catalysts: State of the art and future prospects. *Chem*
1243 *Rev.* 119:10916–10976. <https://doi.org/10.1021/acs.chemrev.9b00202>
- 1244 Han W, Deng J, Xie S, Yang H, Dai H, Au CT (2014) Gold supported on Iron Oxide nanodisk as
1245 efficient catalyst for the removal of toluene. *Ind Eng Chem Res.* 53:3486–3494.
1246 <https://doi.org/10.1021/ie5000505>
- 1247 He C, Li J, Zhang X, Yin L, Chen J, Gao S (2012a) Highly active Pd-based catalysts with
1248 hierarchical pore structure for toluene oxidation: Catalyst property and reaction determining factor.
1249 *Chem Eng J* 180:46–56. <https://doi.org/10.1016/j.cej.2011.10.099>
- 1250 He C, Li P, Wang H, Cheng J, Zhang X, Wang Y, Hao Z (2010) Ligand-assisted preparation of
1251 highly active and stable nanometric Pd confined catalysts for deep catalytic oxidation of toluene.
1252 *J Hazard Mater* 181:996–1003. <http://doi.org/10.1016/j.jhazmat.2010.05.113>
- 1253 He C, Shen Q, Liu M (2014) Toluene destruction over nanometric palladium supported ZSM-5
1254 catalysts: influences of support acidity and operation condition. *J Porous Mater* 21:551–563.
1255 <https://doi.org/10.1007/s10934-014-9802-y>

- 1256 He C, Xu L, Yue L, Chen Y, Chen J, Hao Z (2012b) Supported nanometric Pd hierarchical catalysts
1257 for efficient toluene removal: Catalyst characterization and activity elucidation. *Ind Eng Chem*
1258 *Res* 51:7211–7222. <https://doi.org/10.1021/ie201243c>
- 1259 He C, Zhang F, Yue L, Shang X, Chen J, Hao Z (2012c) Nanometric palladium confined in
1260 mesoporous silica as efficient catalysts for toluene oxidation at low temperature. *Appl Catal B*
1261 *Environ* 111–112:46–57. <http://doi.org/10.1016/j.apcatb.2011.09.017>
- 1262 He J, Balasubramanian R (2008) Rain-aerosol coupling in the tropical atmosphere of Southeast
1263 Asia: Distribution and scavenging ratios of major ionic species. *J Chem* 60(3): 205–220. <https://doi.org/10.1007/s10874-008-9118-x>
- 1265 Hee I, Ji E, Heum C, Wook S, Ook H, Dok Y (2017) Activity of catalysts consisting of Fe₂O₃
1266 nanoparticles decorating entire internal structure of mesoporous Al₂O₃ bead for toluene total
1267 oxidation. *Catal Today* 295:56–64. <http://doi.org/10.1016/j.cattod.2017.03.023>
- 1268 Heidinger B, Royer S, Alamdari H, Giraudon J-M, Lamonier J-F (2019) Reactive grinding
1269 synthesis of LaBO₃ (B: Mn, Fe) perovskite; properties for toluene total oxidation. *Catalysts* 9:633.
1270 <https://doi.org/10.3390/catal9080633>
- 1271 Hoseini S, Rahemi N, Allahyari S, Tasbihi M (2019) Application of plasma technology in the
1272 removal of volatile organic compounds (BTX) using manganese oxide nano-catalysts synthesized
1273 from spent batteries. *J Clean Prod* 232:1134–1147. <https://doi.org/10.1016/j.jclepro.2019.05.227>
- 1274 Hosseini M, Barakat T, Cousin R, Aboukaïs A, Su B, Weireld G De (2012) Catalytic performance
1275 of core-shell and alloy Pd-Au nanoparticles for total oxidation of VOC: The effect of metal
1276 deposition. *Appl Catal B Environ* 112:218–224. <https://doi.org/10.1016/j.apcatb.2011.10.002>
- 1277 Hou Z, Zhou X, Lin T, Chen Y, Lai X, Feng J, Sun M (2019) The promotion effect of tungsten on
1278 monolith Pt/Ce_{0.65}Zr_{0.35}O₂ catalysts for the catalytic oxidation of toluene. *New J Chem* 43:5719–
1279 5726. <https://doi.org/10.1039/C8NJ06245E>
- 1280 Hu F, Chen J, Peng Y, Song H, Li K, Li J (2018) Novel nanowire self-assembled hierarchical CeO₂
1281 microspheres for low temperature toluene catalytic combustion. *Chem Eng J* 331:425–434.
1282 <http://doi.org/10.1016/j.cej.2017.08.110>
- 1283 Hu L, Cheng W, Zhang W, Wu F, Peng S (2017) Monolithic bamboo-based activated carbons for
1284 dynamic adsorption of toluene. *J Porous Mater* 24(2):541–549. <https://doi.org/10.1007/s10934-016-0289-6>
- 1286 Huang H, Gu Y, Zhao J, Wang X (2015) Catalytic combustion of chlorobenzene over VO_x/CeO₂
1287 catalysts. *J Catal* 326:54–68. <http://doi.org/10.1016/j.jcat.2015.02.016>
- 1288 Huang H, Zhang C, Wang L, Li G, Song L, Li G (2016) Promotional effect of HZSM-5 on the
1289 catalytic oxidation of toluene over MnO_x/HZSM-5 catalysts. *Catal Sci Technol* 6:4260–4270.
1290 <https://doi.org/10.1039/C5CY02011E>
- 1291 Huang S, Zhang C, He H (2008) Complete oxidation of o-xylene over Pd/Al₂O₃ catalyst at low
1292 temperature. *Catal Today*. 139:15–23. <https://doi.org/10.1016/j.cattod.2008.08.020>
- 1293 Jardim EDO, Rico-Francés S, Abdelouahab-Feddam Z, Coloma F, Silvestre-Flibero J, Sepúlveda-
1294 Fscribano A, Ramos-Fernandez E V (2015) High performance of Cu/CeO₂-Nb₂O₅ catalysts for

- 1295 preferential CO oxidation and total combustion of toluene. *Applied Catal A, Gen* 502:129–137.
1296 <http://doi.org/10.1016/j.apcata.2015.05.033>
- 1297 Jiang X, Xu W, Lai S, Chen X (2019) Integral structured Co–Mn composite oxides grown on
1298 interconnected Ni foam for catalytic toluene oxidation. *RSC Adv* 9:6533–6541.
1299 <https://doi.org/10.1039/C8RA10102G>
- 1300 Jiang Y, Deng J, Xie S, Yang H, Dai H (2015) Au/MnO_x/3DOM La_{0.6}Sr_{0.4}MnO₃: Highly Active
1301 Nanocatalysts for the Complete Oxidation of Toluene. *Ind Eng Chem Res* 54:900–910.
1302 <https://doi.org/10.1021/ie504304u>
- 1303 Jiang Y, Xie S, Yang H, Deng J, Liu Y, Dai H (2017) Mn₃O₄-Au/3DOM La_{0.6}Sr_{0.4}CoO₃: High-
1304 performance catalysts for toluene oxidation. *Catal Today* 281:437–446.
1305 <http://doi.org/10.1016/j.cattod.2016.05.012>
- 1306 Kamal MS, Razzak SA, Hossain MM (2016) Catalytic oxidation of volatile organic compounds
1307 (VOCs) - A review. *Atmos Environ* 140:117–134. <http://doi.org/10.1016/j.atmosenv.2016.05.031>
- 1308 Kang JS, Sohn Y, Pradhan D, Leung KT (2018) Bimetallic Au@M (M = Ag, Pd, Fe, and Cu)
1309 nanoarchitectures mediated by 1,4-phenylene diisocyanide functionalization. *Langmuir*
1310 34(8):2849–2855. <https://doi.org/10.1021/acs.langmuir.7b02705>
- 1311 Kang S, Hwang J (2020) Fabrication of hollow activated carbon nanofibers (HACNFs) containing
1312 manganese oxide catalyst for toluene removal via two-step process of electrospinning and thermal
1313 treatment. *Chem Eng J* 379:122315. <https://doi.org/10.1016/j.cej.2019.122315>
- 1314 Kim J, Choi M, Ryoo R (2010) Effect of mesoporosity against the deactivation of MFI zeolite
1315 catalyst during the methanol-to-hydrocarbon conversion process. *J Catal* 269:219–228.
1316 <http://doi.org/10.1016/j.jcat.2009.11.009>
- 1317 Kim SC, Jung HY, Nah JW, Park YK (2016) Complete oxidation of toluene over supported
1318 palladium catalysts: effect of support. *J Nanosci Nanotechnol* 16:4638–4642.
1319 <https://doi.org/10.1166/jnn.2016.11020>
- 1320 Lee YE, Chung WC, Chang MB (2019) Photocatalytic oxidation of toluene and isopropanol by
1321 LaFeO₃/black-TiO₂. *Environ Sci Pollut Res* 26:20908–20919. <https://doi.org/10.1007/s11356-019-05436-z>
- 1323 Lerner JEC, Sanchez EY, Sambeth JE, Porta AA (2012) Characterization and health risk
1324 assessment of VOCs in occupational environments in Buenos Aires, Argentina. *Atmos Environ*
1325 55:440–447. <http://doi.org/10.1016/j.atmosenv.2012.03.041>
- 1326 Li J, Qu Z, Qin Y, Wang H (2016) Effect of MnO₂ morphology on the catalytic oxidation of
1327 toluene over Ag/MnO₂ catalysts. *Appl Surf Sci* 385:234–240.
1328 <https://doi.org/10.1016/j.apsusc.2016.05.114>
- 1329 Li L, Zhang F, Zhong Z, Zhu M, Jiang C, Hu J, Xing W (2017) Novel synthesis of a high-
1330 performance Pt/ZnO/SiC filter for the oxidation of toluene. *Ind Eng Chem Res* 56:13857–13865.
1331 <https://doi.org/10.1021/acs.iecr.7b02793>
- 1332 Li WB, Wang JX, Gong H (2009) Catalytic combustion of VOCs on non-noble metal catalysts.
1333 *Catal Today* 148:81–87. <https://doi.org/10.1016/j.cattod.2009.03.007>

- 1334 Li Y, Li W, Liu F, Li M, Qi X, Xue M, Wang Y, Han F (2020) Construction of CeO₂/TiO₂
1335 heterojunctions immobilized on activated carbon fiber and its synergetic effect between adsorption
1336 and photodegradation for toluene removal. *J Nanoparticle Res* 22:122.
1337 <https://doi.org/10.1007/s11051-020-04860-4>
- 1338 Li Y, Liu F, Fan Y, Cheng G, Song W, Zhou J (2018) Silver palladium bimetallic core-shell
1339 structure catalyst supported on TiO₂ for toluene oxidation. *Appl Surf Sci* 462:207–212.
1340 <https://doi.org/10.1016/j.apsusc.2018.08.023>
- 1341 Li YW, Ma WL (2021) Photocatalytic oxidation technology for indoor air pollutants elimination:
1342 A review. *Chemosphere* 280:130667. <https://doi.org/10.1016/j.chemosphere.2021.130667>
- 1343 Lin Y, Minghua H, Jvcheng, Xu Z (2018) Catalytic oxidation of toluene over Co-modified
1344 manganese oxide octahedral molecular sieves (OMS-2) synthesized by different methods. *Mater*
1345 *Sci Eng* 392:032017. <https://doi.org/10.1088/1757-899X/392/3/032017>
- 1346 Liotta LF (2014) New trends in gold catalysts. *Catalysts* 4:299–304.
1347 <https://doi.org/10.3390/catal4030299>
- 1348 Liu C, Lin T, Chan SI, Mou C (2015) A room temperature catalyst for toluene aliphatic C–H bond
1349 oxidation: Tripodal tridentate copper complex immobilized in mesoporous silica. *J Catal* 322:139–
1350 151. <http://doi.org/10.1016/j.jcat.2014.12.005>
- 1351 Liu L, Jia J, Sun T, Zhang H (2018) A facile method for scalable preparation of mesoporous
1352 structured SmMnO₃ perovskites sheets for efficient catalytic oxidation of toluene. *Mater Lett*
1353 212:107–110. <https://doi.org/10.1016/j.matlet.2017.10.048>
- 1354 Liu L, Song Y, Fu Z, Ye Q, Cheng S, Kang T, Dai H (2017) Effect of preparation method on the
1355 surface characteristics and activity of the Pd/OMS-2 catalysts for the oxidation of carbon
1356 monoxide, toluene, and ethyl acetate. *Appl Surf Sci* 396:599–608.
1357 <http://doi.org/10.1016/j.apsusc.2016.10.202>
- 1358 Liu L, Sun J, Ding J, Zhang Y, Jia J, Sun T (2019a) Catalytic Oxidation of VOCs over SmMnO₃
1359 Perovskites: Catalyst Synthesis, Change Mechanism of Active Species, and Degradation Path of
1360 Toluene. *Inorg Chem* 58:14275–14283. <https://doi.org/10.1021/acs.inorgchem.9b02518>
- 1361 Liu L, Sun J, Ding J, Zhang Y, Sun T, Jia J (2019b) Highly active Mn_{3–x}Fe_xO₄ spinel with defects
1362 for toluene mineralization: Insights into regulation of the oxygen vacancy and active metals. *Inorg*
1363 *Chem* 58:13241–13249. <https://doi.org/10.1021/acs.inorgchem.9b02105>
- 1364 Liu P, He H, Wei G, Liu D, Liang X, Chen T, Zhu J, Zhu R (2017) An efficient catalyst of
1365 manganese supported on diatomite for toluene oxidation: Manganese species, catalytic
1366 performance, and structure-activity relationship. *Microporous Mesoporous Mater* 239:101–110.
1367 <http://doi.org/10.1016/j.micromeso.2016.09.053>
- 1368 Liu X, Wang J, Zeng J, Wang X, Zhu T (2015) Catalytic oxidation of toluene over a porous Co₃O₄-
1369 supported ruthenium catalyst. *RSC Adv* 5:52066–52071. <https://doi.org/10.1039/C5RA07072D>
- 1370 Liu Y, Liu Y, Guo Y, Xu J, Xu X, Fang X, Liu J, Chen W, Arandiyani H, Wang X (2018) Tuning
1371 SnO₂ surface area for catalytic toluene deep oxidation: On the inherent factors determining the
1372 reactivity. *Ind Eng Chem Res* 57:14052–14063. <https://doi.org/10.1021/acs.iecr.8b03401>

- 1373 Liu Z, Chen J, Peng Y (2013) Activated carbon fibers impregnated with Pd and Pt catalysts for
1374 toluene removal. *J Hazard Mater* 256–257:49–55. <http://doi.org/10.1016/j.jhazmat.2013.04.007>
- 1375 Lu A, Sun H, Zhang N, Che L, Shan S, Luo J, Zheng J, Yang L, Peng D, Zhong C, Chen B (2019)
1376 Surface Partial-Charge-Tuned enhancement of catalytic activity of platinum nanocatalysts for
1377 toluene oxidation. *ACS Catal* 9:7431–7442. <https://doi.org/10.1021/acscatal.9b01776>
- 1378 Luo M, Cheng Y, Peng X, Pan W (2019) Copper modified manganese oxide with tunnel structure
1379 as efficient catalyst for low-temperature catalytic combustion of toluene. *Chem Eng J* 369:758–
1380 765. <https://doi.org/10.1016/j.cej.2019.03.056>
- 1381 Luo Y, Zheng Y, Zuo J, Feng X, Wang X, Zhang T (2018) Insights into the high performance of
1382 Mn-Co oxides derived from metal-organic frameworks for total toluene oxidation. *J Hazard Mater*
1383 349:119–127. <https://doi.org/10.1016/j.jhazmat.2018.01.053>
- 1384 Lv L, Wang S, Ding Y, Zhang L, Gao Y, Wang S (2020) Deactivation mechanism and anti-
1385 deactivation modification of Ru/TiO₂ catalysts for CH₃Br oxidation. *Chemosphere* 257:127249.
1386 <https://doi.org/10.1016/j.chemosphere.2020.127249>
- 1387 Lyu Y, Li C, Du X, Zhu Y, Zhang Y, Li S (2020) Catalytic removal of toluene over manganese
1388 oxide-based catalysts: a review. *Environ Sci Pollut Res* 27:2482–2501.
1389 <https://doi.org/10.1007/s11356-019-07037-2>
- 1390 Ma J, Yu J, Chen W, Zeng A (2016) The effect of water on the oxidation of toluene catalyzed by
1391 molybdenum manganese complex oxide. *Catal Letters* 146(8):1600–1610.
1392 <https://doi.org/10.1007/s10562-016-1780-z>
- 1393 Magnoux P, Guisnet M (1999) Catalytic oxidation of volatile organic compounds 1.Oxidation of
1394 xylene over a 0.2wt% Pd/HFAU(17) catalyst. *Appl Catal B Environ* 20:1–13.
1395 [https://doi.org/10.1016/S0926-3373\(98\)00087-3](https://doi.org/10.1016/S0926-3373(98)00087-3)
- 1396 Mekki A, Boukoussa B (2019) Structural, textural and toluene adsorption properties of
1397 microporous-mesoporous zeolite omega synthesized by different methods. *J Mater Sci*
1398 54(11):8096–8107. <https://doi.org/10.1007/s10853-019-03450-7>
- 1399 Meng Q, Wang W, Weng X, Liu Y, Wang H, Wu Z (2016) Active oxygen species in La_{n+1}Ni_nO_{3n+1}
1400 layered perovskites for catalytic oxidation of toluene and methane. *J Phys Chem C* 120:3259–3266.
1401 <https://doi.org/10.1021/acs.jpcc.5b08703>
- 1402 Mills A, O'Rourke C (2012) Photocatalytic oxidation of toluene in an NMR tube. *J Photochem*
1403 *Photobiol A Chem* 233:34–39. <http://doi.org/10.1016/j.jphotochem.2012.02.001>
- 1404 Molina R, Moreno S, Haidy M (2017) Effect of Mg and Al on manganese oxides as catalysts for
1405 VOC oxidation. *Mol Catal* 443:117–124. <https://doi.org/10.1016/j.mcat.2017.09.015>
- 1406 Narayanan S, Vijaya JJ, John SSL (2015) Synthesis of hierarchical ZSM-5 hexagonal cubes and
1407 their catalytic activity in the solvent-free selective oxidation of toluene. *J Porous Mater*:907–918.
1408 <https://doi.org/10.1007/s10934-015-9964-2>
- 1409 Nie L, Zhou P, Yu J, Jaroniec M (2014) Deactivation and regeneration of Pt/TiO₂ nanosheet-type
1410 catalysts with exposed (001) facets for room temperature oxidation of formaldehyde. *J Mol Catal*
1411 *A Chem* 390:7–13. <http://doi.org/10.1016/j.molcata.2014.02.033>

- 1412 Niu J, Qian H, Liu J, Liu H, Zhang P, Duan E (2018) Process and mechanism of toluene oxidation
1413 using $\text{Cu}_{1-y}\text{Mn}_2\text{Ce}_y\text{O}_x$ /sepiolite prepared by the co-precipitation method. *J Hazard Mater* 357:332–
1414 340. <https://doi.org/10.1016/j.jhazmat.2018.06.004>
- 1415 Nunotani N, Saeki S, Matsuo K, Imanaka N (2020) Novel catalysts based on lanthanum
1416 oxyfluoride for toluene combustion. *Mater Lett* 258:126802.
1417 <https://doi.org/10.1016/j.matlet.2019.126802>
- 1418 Okumura K, Kobayashi T, Tanaka H, Niwa M (2003) Toluene combustion over palladium
1419 supported on various metal oxide supports. *Appl Catal B Environ.* 44:325–331.
1420 [https://doi.org/10.1016/S0926-3373\(03\)00101-2](https://doi.org/10.1016/S0926-3373(03)00101-2)
- 1421 Okumura K, Amano J, Yasunobu N, Niwa M (2000) X-ray Absorption Fine Structure Study of the
1422 Formation of the Highly Dispersed PdO over ZSM-5 and the Structural Change of Pd Induced by
1423 Adsorption of NO. *J Phys Chem B.* 104: 1050–1057. <https://doi.org/10.1021/jp993182w>
- 1424 Pan J, Du W, Liu Y, Cheng Y, Yuan S (2019) Lanthanum-doped Cu-Mn composite oxide catalysts
1425 for catalytic oxidation of toluene. *J Rare Earths* 37(6):602–608.
1426 <https://doi.org/10.1016/j.jre.2018.10.004>
- 1427 Pan KL, Chang MB (2019) Plasma catalytic oxidation of toluene over double perovskite-type
1428 oxide via packed-bed DBD. *Environ Sci Pollut Res* 26:12948–12962.
1429 <https://doi.org/10.1007/s11356-019-04714-0>
- 1430 Parsafard N, Peyrovi MH, Shokoohi MV (2018) Study of HMS modified ZrO_2 supported platinum
1431 catalysts for toluene removal: Catalytic combustion and kinetics study. *Phys Chem Res* 6:721–
1432 728. <https://doi.org/10.22036/pcr.2018.141366.1508>
- 1433 Peedikakkal AMP, Jimoh AA, Shaikh MN, Ali B El (2017) Mixed-metal metal-organic
1434 frameworks as catalysts for liquid-phase oxidation of toluene and cycloalkanes. *Arab J Sci Eng*
1435 42:4383–4390. <https://doi.org/10.1007/s13369-017-2452-z>
- 1436 Peng H, Dong T, Zhang L, Wang C, Liu W, Bao J, Wang X (2019) Active and stable Pt-Ceria
1437 nanowires@silica shell catalyst: Design, formation mechanism and total oxidation of CO and
1438 toluene. *Appl Catal B Environ* 256:117807. <https://doi.org/10.1016/j.apcatb.2019.117807>
- 1439 Peng R, Li S, Sun X, Ren Q, Chen L, Fu M, Wu J, Ye D (2018) Size effect of Pt nanoparticles on
1440 the catalytic oxidation of toluene over Pt/ CeO_2 catalysts. *Appl Catal B Environ* 220:462–470.
1441 <http://doi.org/10.1016/j.apcatb.2017.07.048>
- 1442 Peng R, Sun X, Li S, Chen L, Fu M, Wu J, Ye D (2016) Shape effect of Pt/ CeO_2 catalysts on the
1443 catalytic oxidation of toluene. *Chem Eng J* 306:1234–1246.
1444 <http://doi.org/10.1016/j.cej.2016.08.056>
- 1445 Peta S, Zhang T, Dubovoy V, Koh K, Hu M, Wang X, Asefa T (2018) Facile synthesis of efficient
1446 and selective Ti-containing mesoporous silica catalysts for toluene oxidation. *Mol Catal* 444:34–
1447 41. <https://doi.org/10.1016/j.mcat.2017.10.007>
- 1448 Pinard L, Tayeb K Ben, Hamieh S, Vezin H, Canaff C, Maury S, Delpoux O, Pouilloux Y (2013)
1449 On the involvement of radical “coke” in ethanol conversion to hydrocarbons over HZSM-5 zeolite.
1450 *Catal Today* 218–219:57–64. <http://doi.org/10.1016/j.cattod.2013.03.039>

- 1451 Qiao N, Li Y, Li N, Zhang X, Cheng J, Hao Z (2015) High performance Pd catalysts supported on
1452 bimodal mesopore silica for the catalytic oxidation of toluene. *Chinese J Catal* 36(10):1686–1693.
1453 [https://doi.org/10.1016/S1872-2067\(15\)60924-X](https://doi.org/10.1016/S1872-2067(15)60924-X)
- 1454 Qin L, Huang X, Zhao B, Wang Y, Han J (2019) Iron oxide as a promoter for toluene catalytic
1455 oxidation over Fe–Mn/ γ -Al₂O₃ catalysts. *Catal Letters* (0123456789).
1456 <https://doi.org/10.1007/s10562-019-02975-5>
- 1457 Qin Y, Qu Z, Dong C, Huang N (2017) Effect of pretreatment conditions on catalytic activity of
1458 Ag/SBA-15 catalyst for toluene oxidation. *Chinese J Catal* 38(9):1603–1612.
1459 [http://doi.org/10.1016/S1872-2067\(17\)62842-0](http://doi.org/10.1016/S1872-2067(17)62842-0)
- 1460 Qin Y, Qu Z, Dong C, Wang Y, Huang N (2018) Highly catalytic activity of Mn/SBA-15 catalysts
1461 for toluene combustion improved by adjusting the morphology of supports. *J Environ Sci* 76:208–
1462 216. <https://doi.org/10.1016/j.jes.2018.04.027>
- 1463 Qiu L, Wang Y, Li H, Cao G, Ouyang F, Zhu R (2018) Photocatalytic oxidation of toluene on
1464 fluorine doped TiO₂/SiO₂ catalyst under simulant sunlight in a flat reactor. *Catalysts* 8:596.
1465 <https://doi.org/10.3390/catal8120596>
- 1466 Ren Q, Feng Z, Mo S, Huang C, Li S, Zhang W (2019) 1D-Co₃O₄, 2D-Co₃O₄, 3D-Co₃O₄ for
1467 catalytic oxidation of toluene. *Catal Today* 332:160–167.
1468 <https://doi.org/10.1016/j.cattod.2018.06.053>
- 1469 Ren Q, Mo S, Peng R, Feng Z, Zhang M (2018) Controllable synthesis of 3D hierarchical Co₃O₄
1470 nanocatalysts with various morphologies for the catalytic oxidation of toluene. *J Mater Chem A*
1471 6:498–509. <https://doi.org/10.1039/C7TA09149D>
- 1472 Reza S, Pirsaraei A, Asilian H, Ahmad M, Jafari J (2016) Airborne toluene degradation by using
1473 manganese oxide supported on a modified natural diatomite. *J Porous Mater* 23:1015–1024.
1474 <https://doi.org/10.1007/s10934-016-0159-2>
- 1475 Rokici A, Drozdek M, Dudek B, Gil B, Michoreczyk P, Brouri D, Dzwigaj S, Ku P (2017) Cobalt-
1476 containing BEA zeolite for catalytic combustion of toluene. *Appl Catal B Environ* 212:59–67.
1477 <https://doi.org/10.1016/j.apcatb.2017.04.067>
- 1478 Rokici A, Natka P, Dudek B, Drozdek M, Lity L, Ku P (2016) Co₃O₄-pillared montmorillonite
1479 catalysts synthesized by hydrogel-assisted route for total oxidation of toluene. *Appl Catal B*
1480 *Environ* 195:59–68. <https://doi.org/10.1016/j.apcatb.2016.05.008>
- 1481 Romero D, Chlala D, Labaki M, Royer S, Bellat J, Bezverkhyy I, Giraudon J, Lamonier J (2015)
1482 Removal of toluene over NaX zeolite exchanged with Cu²⁺. *Catalysts* 5:1479–1497.
1483 <https://doi.org/10.3390/catal5031479>
- 1484 Rui Z, Tang M, Ji W, Ding J, Ji H (2017) Insight into the enhanced performance of TiO₂ nanotube
1485 supported Pt catalyst for toluene oxidation. *Catal Today* 297:159–166.
1486 <http://doi.org/10.1016/j.cattod.2017.04.055>
- 1487 Ryu HW, Song MY, Park JS, Kim JM, Jung SC, Song J, Kim BJ, Part YK (2019) Removal of
1488 toluene using ozone at room temperature over mesoporous Mn/Al₂O₃ catalysts. *Environ Res*
1489 172:649–657. <https://doi.org/10.1016/j.envres.2019.03.016>

- 1490 Sanchis R, Alonso-dom D, Dejoz A (2018) Eco-friendly cavity-containing Iron oxides prepared
1491 by mild routes as very efficient catalysts for the total oxidation of VOCs. *Materials* 11:1387.
1492 <https://doi.org/10.3390/ma11081387>
- 1493 Santos VP, Carabineiro SAC, Tavares PB, Pereira MFR, Órfão JJM, Figueiredo JL (2010)
1494 Oxidation of CO, ethanol and toluene over TiO₂ supported noble metal catalysts. *Appl Catal B,*
1495 *Environ* 99:198–205. <http://doi.org/10.1016/j.apcatb.2010.06.020>
- 1496 Sedjame H, Fontaine C, Lafaye G, Jr JB (2014) On the promoting effect of the addition of ceria to
1497 platinum based alumina catalysts for VOCs oxidation. *Appl Catal B, Environ* 144:233–242.
1498 <http://doi.org/10.1016/j.apcatb.2013.07.022>
- 1499 Si W, Wang Y, Zhao S, Hu F, Li J (2016) A facile method for in Situ preparation of the
1500 MnO₂/LaMnO₃ catalyst for the removal of toluene. *Environ Sci Technol* 50:4572–4578.
1501 <https://doi.org/10.1021/acs.est.5b06255>
- 1502 Sihaib Z, Puleo F, Garcia-Vargas JM, Retailleau L, Descorme C, Liotta LF, Valverde JL, Gil S,
1503 Giroir-Fendler A (2017) Manganese oxide-based catalysts for toluene oxidation. *Appl Catal, B*
1504 209:689–700. <https://doi.org/10.1016/j.apcatb.2017.03.042>
- 1505 Song M, Yu L, Song B, Meng F, Tang X (2019) Alkali promoted the adsorption of toluene by
1506 adjusting the surface properties of lignin-derived carbon fibers. *Environ Sci Pollut Res* 26:22284–
1507 22294. <https://doi.org/10.1007/s11356-019-05456-9>
- 1508 Spivey JJ (1987) Complete catalytic oxidation of volatile organics. *Ind Eng Chem Res* 26:2165–
1509 2180. <https://doi.org/10.1021/ie00071a001>
- 1510 Suárez-vázquez SI, Gil S, García-vargas JM, Cruz-lópez A, Giroir-fendler A (2018) Catalytic
1511 oxidation of toluene by SrTi_{1-x}B_xO₃ (B=Cu and Mn) with dendritic morphology synthesized by
1512 one pot hydrothermal route. *Applied Catal B, Environ* 223:201–208.
1513 <http://doi.org/10.1016/j.apcatb.2017.04.042>
- 1514 Sun H, Yu X, Yang X, Ma X, Lin M, Shao C (2019a) Au/Rod-like MnO₂ catalyst via thermal
1515 decomposition of manganite precursor for the catalytic oxidation of toluene. *Catal Today* 332:153–
1516 159. <https://doi.org/10.1016/j.cattod.2018.07.017>
- 1517 Sun H, Yu X, Ma X, Yang X, Lin M, Ge M (2019b) MnO_x-CeO₂ catalyst derived from metal-
1518 organic frameworks for toluene oxidation. *Catal Today* 355:580-586.
1519 <https://doi.org/10.1016/j.cattod.2019.05.062>
- 1520 Sun R, Shi Q, Zhang M, Xie L, Chen J, Yang X, Chen M, Zhao W (2017) Enhanced photocatalytic
1521 oxidation of toluene with a coral-like direct Z-scheme BiVO₄/g-C₃N₄ photocatalyst. *J Alloys*
1522 *Compd* 714:619–626. <http://doi.org/10.1016/j.jallcom.2017.04.108>
- 1523 Sun Y, He J, Yang G, Sun G, Sage V (2019c) A review of the enhancement of bio-hydrogen
1524 generation by chemicals addition. *Catalysts* 9(4): 353. <https://doi.org/10.3390/catal9040353>
- 1525 Tan W, Deng J, Xie S, Yang H, Jiang Y, Guo G, Dai H (2015) Ce_{0.6}Zr_{0.3}Y_{0.1}O₂ nanorod supported
1526 gold and palladium alloy nanoparticles: high-performance catalysts for toluene oxidation.
1527 *Nanoscale* 7:8510–8523.
- 1528 Tanada S, Kawasaki N, Nakamura T, Araki M, Isomura M (1999) Removal of Formaldehyde by

- 1529 Activated Carbons Containing Amino Groups. *J Colloid Interface Sci* 214:106–108.
1530 <https://doi.org/10.1006/jcis.1999.6176>
- 1531 Tarjomannejad A, Farzi A, Niaei A, Salari D (2016) An experimental and kinetic study of toluene
1532 oxidation over $\text{LaMn}_{1-x}\text{B}_x\text{O}_3$ and $\text{La}_{0.8}\text{A}_{0.2}\text{Mn}_{0.3}\text{B}_{0.7}\text{O}_3$ (A=Sr, Ce and B=Cu, Fe) nano-perovskite
1533 catalysts. *Korean J Chem Eng.* 33:2628–2637. <https://doi.org/10.1007/s11814-016-0108-4>
- 1534 Thanh N, Le M, Thanh D, Cong B, Ngo T, An T, Quang N (2018) Dual functional
1535 adsorbent/catalyst of nano-gold/metal oxides supported on carbon grain for low-temperature
1536 removal of toluene in the presence of water vapor. *Clean Technol Environ Policy* 20:1861–1873.
1537 <https://doi.org/10.1007/s10098-018-1583-6>
- 1538 Tian Y, Liu W, Lu Y, Sun S (2016) Molten salt synthesis of strontium-doped Lanthanum
1539 manganite nanoparticles with enhanced catalytic performance for toluene combustion. *Nano* 11:1–
1540 9. <https://doi.org/10.1142/S1793292016500594>
- 1541 Tomatis M, Xu HH, He J, Zhang XD (2016) Recent development of catalysts for removal of
1542 volatile organic compounds in flue gas by combustion: A review. *J Chem* 2016.
1543 <https://doi.org/10.1155/2016/8324826>
- 1544 Tomatis M, Moreira M, Xu HH, Deng W, He J, Parvez AM (2019) Removal of VOCs from waste
1545 gases using various thermal oxidizers: A comparative study based on life cycle assessment and
1546 cost analysis in China. *J Clean Prod* 233: 808-818. <https://doi.org/10.1016/j.jclepro.2019.06.131>
- 1547 Torrente-murciano L, Solsona B, Agouram S, Sanchis R (2017) Low temperature total oxidation
1548 of toluene by bimetallic Au–Ir catalysts. *Catal Sci Technol* 7:2886–2896.
1549 <https://doi.org/10.1039/C7CY00635G>
- 1550 Uzuki TS, Hiono KS, Anabe SM, Abe TY, Igo TH, Go SO, Ekine YS (2018) Selective adsorption
1551 of toluene on perovskite-type oxide. *J Japan Pet Inst* 61:272–281.
1552 <https://doi.org/10.1627/jpi.61.272>
- 1553 Wang H, Yang W, Tian P, Zhou J, Tang R, Wu S (2017a) A highly active and anti-coking Pd-
1554 Pt/SiO₂ catalyst for catalytic combustion of toluene at low temperature. *Appl Catal A, Gen* 529:60–
1555 67. <http://doi.org/10.1016/j.apcata.2016.10.016>
- 1556 Wang H, Lu Y, Han Y, Lu C, Wan H, Xu Z, Zheng S (2017b) Enhanced catalytic toluene oxidation
1557 by interaction between copper oxide and manganese oxide in Cu-O-Mn/Al₂O₃ catalysts. *Appl Surf*
1558 *Sci* 420:260–266. <http://doi.org/10.1016/j.apsusc.2017.05.133>
- 1559 Wang J, Zhang P, Li J, Jiang C, Yunus R, Kim J (2015) Room-temperature oxidation of
1560 formaldehyde by layered manganese oxide: Effect of water. *Environ Sci Technol* 49:12372–12379.
1561 <https://doi.org/10.1021/acs.est.5b02085>
- 1562 Wang L, Zhang C, Huang H (2016) Catalytic oxidation of toluene over active MnO_x catalyst
1563 prepared via an alkali-promoted redox precipitation method. *React Kinet Mech Catal* 118:605–
1564 619. <https://doi.org/10.1007/s11144-016-1011-z>
- 1565 Wang WL, Meng Q, Weng X, Wu Z (2016) Rapid syntheses of ultrafine LaMnO₃ nano-crystallites
1566 with superior activity for catalytic oxidation of toluene. *Catal Commun* 84:167–170.
1567 <http://doi.org/10.1016/j.catcom.2016.06.030>

- 1568 Wang X, Choi S Il, Roling LT, Luo M, Ma C, Zhang L, Chi M, Liu J, Xie Z, Herron JA, et al
1569 (2015) Palladium-platinum core-shell icosahedra with substantially enhanced activity and
1570 durability towards oxygen reduction. *Nat Commun* 118:605-619.
1571 <https://doi.org/10.1038/ncomms8594>
- 1572 Wang Y, Arandiyan H, Liu Y, Liang Y, Peng Y, Bartlett S, Dai H, Rostamnia S, Li J (2018)
1573 Template-free scalable synthesis of flower-like $\text{Co}_{3-x}\text{Mn}_x\text{O}_4$ spinel catalysts for toluene oxidation.
1574 *ChemCatChem* 10:3429–3434. <https://doi.org/10.1002/cctc.201800598>
- 1575 Wang Z, Liu Y, Yang T, Deng J, Xie S, Dai H (2017) Catalytic performance of cobalt oxide-
1576 supported gold-palladium nanocatalysts for the removal of toluene and o-xylene. *Chinese J Catal*
1577 38:207–216. [http://doi.org/10.1016/S1872-2067\(16\)62569-X](http://doi.org/10.1016/S1872-2067(16)62569-X)
- 1578 Wang Z, Xie Y, Liu C (2008) Synthesis and characterization of noble metal (Pd, Pt, Au, Ag)
1579 nanostructured materials confined in the channels of mesoporous SBA-15. *J Phys Chem C*
1580 12:19818–19824. <https://doi.org/10.1021/jp805538j>
- 1581 Wei G, Zhang Q, Zhang D, Wang J, Tang T, Wang H, Liu X (2019) The influence of annealing
1582 temperature on copper-manganese catalyst towards the catalytic combustion of toluene: The
1583 mechanism study. *Appl Surf Sci* 497:143777. <https://doi.org/10.1016/j.apsusc.2019.143777>
- 1584 Wei Y, Ni L, Li M, Zhao J (2017) A template-free method for preparation of MnO_2 catalysts with
1585 high surface areas. *Catal Today* 297:188–192. <https://doi.org/10.1016/j.cattod.2016.12.044>
- 1586 Weng X, Shi B, Liu A, Sun J, Xiong Y, Wan H, Zheng S, Dong L, Chen Y (2019) Highly dispersed
1587 Pd/modified- Al_2O_3 catalyst on complete oxidation of toluene: Role of basic sites and mechanism
1588 insight. *Appl Surf Sci* 497:143747. <https://doi.org/10.1016/j.apsusc.2019.143747>
- 1589 Weng X, Wang WL, Meng Q, Wu Z (2018) An ultrafast approach for the syntheses of defective
1590 nanosized lanthanide perovskites for catalytic toluene oxidation. *Catal Sci Technol* 8(17):4364–
1591 4372. <https://doi.org/10.1039/C8CY01000E>
- 1592 Tang WX, Wu XF, Liu G, Li SD, Li DY, Li WH, Chen YF (2015) Preparation of hierarchical
1593 layer-stacking Mn-Ce composite oxide for catalytic total oxidation of VOCs. *J Rare Earths* 33:62–
1594 69. [http://doi.org/10.1016/S1002-0721\(14\)60384-7](http://doi.org/10.1016/S1002-0721(14)60384-7)
- 1595 Ryu HW, Song MY, Par JS, Kim JM, Jung SC, Song JH, Kim BJ, Part YK (2019) Removal of
1596 toluene using ozone at room temperature over mesoporous Mn/ Al_2O_3 catalysts. *Environ Res*
1597 172:649–657. <https://doi.org/10.1016/j.envres.2019.03.016>
- 1598 Wook S, Geun M, Hee I, Ook H, Dok Y (2016) Use of NiO/ SiO_2 catalysts for toluene total
1599 oxidation: Catalytic reaction at lower temperatures and repeated regeneration. *Chinese J Catal*
1600 37:1931–1940. [http://doi.org/10.1016/S1872-2067\(16\)62514-7](http://doi.org/10.1016/S1872-2067(16)62514-7)
- 1601 Wu J, Sun W, Cao L, Yang J (2016) Removal of highly concentrated toluene from flue gas by an
1602 anode-supported solid oxide fuel cell reactor to generate electricity. *Chem Eng J* 301:334–341.
1603 <http://dx.doi.org/10.1016/j.cej.2016.04.146>
- 1604 Wu JC, Chang T (1998) VOC deep oxidation over Pt catalysts using hydrophobic supports. *Catal*
1605 *Today* 44:111–118. [https://doi.org/10.1016/S0920-5861\(98\)00179-5](https://doi.org/10.1016/S0920-5861(98)00179-5)
- 1606 Wu M, Chen S, Soomro A, Ma S, Zhu M, Hua X, Xiang W (2019a) Investigation of synergistic

- 1607 effects and high performance of La-Co composite oxides for toluene catalytic oxidation at low
1608 temperature. *Environ Sci Pollut Res* 26:12123–12135. [https://doi.org/10.1007/s11356-019-04672-](https://doi.org/10.1007/s11356-019-04672-7)
1609 7
- 1610 Wu M, Zhang Y, Szeto W, Pan W, Huang H, Leung DYC (2019b) Vacuum ultraviolet (VUV)-
1611 based photocatalytic oxidation for toluene degradation over pure CeO₂. *Chem Eng Sci* 200:203–
1612 213. <https://doi.org/10.1016/j.ces.2019.01.056>
- 1613 Wu Z, Deng J, Xie S, Yang H, Zhao X, Zhang K, Lin H, Dai H, Guo G (2016) Mesoporous Cr₂O₃-
1614 supported AuPd nanoparticles: High-performance catalysts for the oxidation of toluene.
1615 *Microporous Mesoporous Mater* 224:311–322. <http://doi.org/10.1016/j.micromeso.2015.11.061>
- 1616 Wu Z, Zhang L, Guan Q, Fu M, Ye D, Wu T (2015) Catalytic oxidation of toluene over Au–Co
1617 supported on SBA-15. *Mater Res Bull* 70:567–572.
1618 <http://doi.org/10.1016/j.materresbull.2015.05.028>
- 1619 Xia Y, Lin M, Ren D, Li Y, Hu F (2017) Preparation of high surface area mesoporous nickel oxides
1620 and catalytic oxidation of toluene and formaldehyde. *J Porous Mater* 24(3):621–629.
1621 <https://doi.org/10.1007/s10934-016-0298-5>
- 1622 Zhang XD, Wang Y, Yang YQ, Chen D (2015) Recent progress in the removal of volatile organic
1623 compounds by mesoporous silica materials and supported catalysts. *Acta Phy Chim Sin* 31:1633–
1624 1646. <https://doi.org/10.3866/PKU.WHXB201507281>
- 1625 Xiao H, Wu J, Wang X, Wang J, Mo S, Fu M (2018) Ozone-enhanced deep catalytic oxidation of
1626 toluene over a platinum-ceria- supported BEA zeolite catalyst. *Mol Catal* 460:7–15.
1627 <https://doi.org/10.1016/j.mcat.2018.09.005>
- 1628 Xie R, Ji J, Huang H, Lei D, Fang R, Shu Y, Zhan Y, Guo K, Leung DYC (2018) Heterogeneous
1629 activation of peroxymonosulfate over monodispersed Co₃O₄/activated carbon for efficient
1630 degradation of gaseous toluene. *Chem Eng J* 341:383–391.
1631 <https://doi.org/10.1016/j.cej.2018.02.045>
- 1632 Xie R, Lei D, Zhan Y, Liu B, Tsang CHA, Zeng Y, Li K, Leung DYC, Huang H (2020) Efficient
1633 photocatalytic oxidation of gaseous toluene over F-doped TiO₂ in a wet scrubbing process. *Chem*
1634 *Eng J* 386:121025. <https://doi.org/10.1016/j.cej.2019.02.112>
- 1635 Xie S, Deng J, Zang S, Yang H, Guo G, Arandiyani H, Dai H (2015a) Au–Pd/3DOM Co₃O₄: Highly
1636 active and stable nanocatalysts for toluene oxidation. *J Catal* 322:38–48.
1637 <http://doi.org/10.1016/j.jcat.2014.09.024>
- 1638 Xie S, Deng J, Liu Y, Zhang Z, Yang H, Jiang Y (2015b) Excellent catalytic performance, thermal
1639 stability, and water resistance of 3DOM Mn₂O₃-supported Au–Pd alloy nanoparticles for the
1640 complete oxidation of toluene. *Appl Catal A, Gen* 507:82–90.
1641 <http://doi.org/10.1016/j.apcata.2015.09.026>
- 1642 Xu J, Tai XH, Betha R, He J, Balasubramanian R (2015a) Comparison of physical and chemical
1643 properties of ambient aerosols during the 2009 haze and non-haze periods in Southeast Asia.
1644 *Environ Geochem Health* 37(5): 831–841. <https://doi.org/10.1007/s10653-014-9667-7>
- 1645 Xu Z, Yu J, Jaroniec M (2015b) Efficient catalytic removal of formaldehyde at room temperature

- 1646 using AlOOH nanoflakes with deposited Pt. *Appl Catal B Environ* 163:306–312.
1647 <http://doi.org/10.1016/j.apcatb.2014.08.017>
- 1648 Yang J, Li L, Yang X, Song S, Li J, Jing F, Chu W (2019a) Enhanced catalytic performances of
1649 in situ-assembled LaMnO₃/δ-MnO₂ hetero-structures for toluene combustion. *Catal Today*
1650 327:19–27. <https://doi.org/10.1016/j.cattod.2018.07.040>
- 1651 Yang C, Miao G, Pi Y, Xia Q, Wu J, Li Z, Xiao J (2019b) Abatement of various types of VOCs
1652 by adsorption/catalytic oxidation: A review. *Chem Eng J* 370:1128–1153.
1653 <https://doi.org/10.1016/j.cej.2019.03.232>
- 1654 Yang H, Deng J, Liu Y, Xie S, Wu Z, Dai H (2016a) Preparation and catalytic performance of Ag,
1655 Au, Pd or Pt nanoparticles supported on 3DOM CeO₂-Al₂O₃ for toluene oxidation. "Journal Mol
1656 Catal A, Chem 414:9–18. <http://doi.org/10.1016/j.molcata.2015.12.010>
- 1657 Yang H, Deng J, Liu Y, Xie S, Xu P, Dai H (2016b) Pt/Co₃O₄/3DOM Al₂O₃: Highly effective
1658 catalysts for toluene combustion. *Chinese J Catal* 37:934–946. [http://dx.doi.org/10.1016/S1872-2067\(15\)61095-6](http://dx.doi.org/10.1016/S1872-2067(15)61095-6)
- 1660 Yang H, Deng J, Xie S, Jiang Y, Dai H, Tong C (2015a) Au/MnO_x/3DOM SiO₂: Highly active
1661 catalysts for toluene oxidation. *Appl Catal A, Gen* 507:139–148.
1662 <https://doi.org/10.1016/j.apcata.2015.09.043>
- 1663 Yang P, Yang S, Shi Z, Meng Z, Zhou R (2015b) Deep oxidation of chlorinated VOCs over CeO₂-
1664 based transition metal mixed oxide catalysts. *Appl Catal B Environ* 162:227–235.
1665 <http://dx.doi.org/10.1016/j.apcatb.2014.06.048>
- 1666 Yang X, Yu X, Jing M, Song W, Liu J, Ge M (2018a) Defective Mn_xZr_{1-x}O₂ solid solution for the
1667 catalytic oxidation of toluene: Insights into the oxygen vacancy contribution. *ACS Appl Mater*
1668 *Interfaces* 11:730–739. <https://doi.org/10.1021/acsami.8b17062>
- 1669 Yang Q, Wang D, Wang C, Li X, Li K, Peng Y, Li J (2018b) Facile surface improvement method
1670 for LaCoO₃ for toluene oxidation. *Catal Sci Technol.* 8(12):3166–3173.
1671 <https://doi.org/10.1039/C8CY00765A>
- 1672 Yang Y, Liu S, Zhao H, Li H, Qu R, Zhang S, Zhu X, Zheng C, Gao X (2019) Promotional effect
1673 of doping Cu into cerium-titanium binary oxides catalyst for deep oxidation of gaseous
1674 dichloromethane. *Chemosphere* 214:553–562.
1675 <https://doi.org/10.1016/j.chemosphere.2018.09.128>
- 1676 Yao X, Zhang J, Liang X, Long C (2018) Plasma-catalytic removal of toluene over the supported
1677 manganese oxides in DBD reactor: Effect of the structure of zeolites support. *Chemosphere*
1678 208:922–930. <https://doi.org/10.1016/j.chemosphere.2018.06.064>
- 1679 Yin K, Zhang H, Yan Y (2019) High efficiency of toluene adsorption over a novel ZIF-67
1680 membrane coating on paper-like stainless steel fibers. *J Solid State Chem* 279:120976.
1681 <https://doi.org/10.1016/j.jssc.2019.120976>
- 1682 Yu H, Hu W, He J, Ye Z (2019) Decomposition efficiency and aerosol by-products of toluene,
1683 ethyl acetate and acetone using dielectric barrier discharge technique. *Chemosphere* 237: 124439.
1684 <https://doi.org/10.1016/j.chemosphere.2019.124439>

- 1685 Yusuf A, Sun Y, Snape C, He J, Wang C, Ren Y, Jia H (2020a) Low-temperature formaldehyde
1686 oxidation over manganese oxide catalysts: Potassium mediated lattice oxygen mobility. *Mol Catal*
1687 497: 111204. <https://doi.org/10.1016/j.mcat.2020.111204>
- 1688 Yusuf A, Sun Y, Ren Y, Snape C, Wang C, Jia H, He J (2020b) Opposite effects of Co and Cu
1689 dopants on the catalytic activities of birnessite MnO₂ catalysts for low-temperature formaldehyde
1690 oxidation. *J Phys Chem C* 124: 26320-26331.
- 1691 Zang M, Zhao C, Wang Y, Chen S (2019) A review of recent advances in catalytic combustion of
1692 VOCs on perovskite-type catalysts. *J Saudi Chem Soc* 23(6):645–654.
1693 <https://doi.org/10.1016/j.jscs.2019.01.004>
- 1694 Zeng X, Cheng G, Liu Q, Yu W, Yang R, Wu H, Li Y, Sun M, Zhang C, Yu L (2019) Novel
1695 ordered mesoporous γ -MnO₂ catalyst for high-performance catalytic oxidation of toluene and
1696 o-Xylene. *Ind Eng Chem Res* 58:13926–13934. <https://doi.org/10.1021/acs.iecr.9b02087>
- 1697 Zhang Y, Wei C, Yan B (2019a) Emission characteristics and associated health risk assessment of
1698 volatile organic compounds from a typical coking wastewater treatment plant. *Sci Total Environ*
1699 693:133417. <https://doi.org/10.1016/j.scitotenv.2019.07.223>
- 1700 Zhang X, Yang Y, Song L, Chen J, Yang Y, Wang Y (2019b) Enhanced adsorption performance
1701 of gaseous toluene on defective UiO-66 metal organic framework : Equilibrium and kinetic studies.
1702 *J Hazard Mater* 365:597–605. <https://doi.org/10.1016/j.jhazmat.2018.11.049>
- 1703 Zhang X, Zhao J, Song Z, Zhao H, Liu W (2019c) Enhancement of catalytic performance over
1704 different transition metals modified-CeO₂ for toluene abatement. *React Kinet Mech Catal*
1705 128:271–287. <https://doi.org/10.1007/s11144-019-01616-7>
- 1706 Zhang X, Zhao J, Song Z, Zhao H, Liu W (2019d) Cooperative Effect of the Ce–Co–Ox for the
1707 Catalytic Oxidation of Toluene. *Chem Sel.* 4:8902–8909.
- 1708 Zhang Y, Liu Y, Xie S, Huang H, Guo G, Dai H (2019e) Supported ceria-modified silver catalysts
1709 with high activity and stability for toluene removal. *Environ Int* 128:335–342.
1710 <https://doi.org/10.1016/j.envint.2019.04.062>
- 1711 Zhang Y, Si Z, Gao J, Liu Y, Liu L, Wu X, Ran R (2019f) Facile synthesis of NaOH-promoted
1712 Pt/TiO₂ catalysts for toluene oxidation under visible light irradiation. *Appl Surf Sci* 469:246–252.
1713 <https://doi.org/10.1016/j.apsusc.2018.11.060>
- 1714 Zhang Q, Mo S, Chen B, Zhang W, Huang C, Ye D (2018) Hierarchical Co₃O₄ nanostructures in-
1715 situ grown on 3D nickel foam towards toluene oxidation. *Mol Catal* 454:12–20.
1716 <https://doi.org/10.1016/j.mcat.2018.05.006>
- 1717 Zhang Z, Jiang Z, Shangguan W (2016) Low-temperature catalysis for VOCs removal in
1718 technology and application: A state-of-the-art review. *Catal Today* 264:270–278.
1719 <http://doi.org/10.1016/j.cattod.2015.10.040>
- 1720 Zhao B, Jian Y, Jiang Z, Albilali R, He C (2019a) Revealing the unexpected promotion effect of
1721 EuO_x on Pt/CeO₂ catalysts for catalytic combustion of toluene. *Chinese J Catal.* 40:543–552.
1722 [https://doi.org/10.1016/S1872-2067\(19\)63292-4](https://doi.org/10.1016/S1872-2067(19)63292-4)
- 1723 Zhao C, Hao Q, Zhang Q, Yan N, Liu J, Dou B, Bin F (2019b) Catalytic self-sustained combustion

- 1724 of toluene and reaction pathway over $\text{Cu}_x\text{Mn}_{1-x}\text{Ce}_{0.75}\text{Zr}_{0.25}/\text{TiO}_2$ catalysts. *Appl Catal A, Gen.*
1725 569:66–74. <https://doi.org/10.1016/j.apcata.2018.10.034>
- 1726 Zhao J, Dong Z (2018) Enhanced stability of $\text{Pd}/\text{Al}_2\text{O}_3$ during aqueous oxidation reaction via SiH_4
1727 treatment. *J Mater Sci* 53:15795–15803. <https://doi.org/10.1007/s10853-018-2741-2>
- 1728 Zhao J, Tang Z, Dong F, Zhang J (2019c) Controlled porous hollow Co_3O_4 polyhedral nanocages
1729 derived from metal-organic frameworks (MOFs) for toluene catalytic oxidation. *Mol Catal*
1730 463:77–86. <https://doi.org/10.1016/j.mcat.2018.10.020>
- 1731 Zhao J, Xi W, Tu C, Dai Q, Wang X (2020) Catalytic oxidation of chlorinated VOCs over
1732 $\text{Ru}/\text{Ti}_x\text{Sn}_{1-x}$ catalysts. *Appl Catal B Environ* 263:118237.
1733 <https://doi.org/10.1016/j.apcatb.2019.118237>
- 1734 Zhao L, Zhang Z, Li Y, Leng X, Zhang T, Yuan F, Niu X, Zhu Y (2019d) Synthesis of CeMnO_x
1735 hollow microsphere with hierarchical structure and its excellent catalytic performance for toluene
1736 combustion. *Appl Catal B Environ* 245:502–512. <https://doi.org/10.1016/j.apcatb.2019.01.005>
- 1737 Zhu A, Zhou Y, Wang Y, Zhu Q, Liu H, Zhang Z, Lu H (2018a) Catalytic combustion of VOCs
1738 on Pt/CuMnCe and Pt/CeY honeycomb monolithic catalysts. *J Rare Earths* 36:1272–1277.
1739 <https://doi.org/10.1016/j.jre.2018.03.032>
- 1740 Zhu B, Yan Y, Li M, Li X-S, Liu J-L, Zhu Y (2018b) Low temperature removal of toluene over
1741 $\text{Ag}/\text{CeO}_2/\text{Al}_2\text{O}_3$ nanocatalyst in an atmospheric plasma catalytic system. *Plasma Process Polym*
1742 15:1700215. <https://doi.org/10.1002/ppap.201700215>
- 1743 Zhu B, Zhang L, Yan Y, Li M, Zhu Y (2019a) Enhancing toluene removal in a plasma
1744 photocatalytic system through a black TiO_2 photocatalyst. *Plasma Sci Technol* 21:115503.
1745 <https://doi.org/10.1088/2058-6272/ab3668>
- 1746 Zhu J, Andersson SLT (1989) Effect of water on the catalytic oxidation of toluene over vanadium
1747 oxide catalysts. *Appl Catal A, Gen* 53:251–262. [https://doi.org/10.1016/S0166-9834\(00\)80024-X](https://doi.org/10.1016/S0166-9834(00)80024-X)
- 1748 Zhu J, Zhang W, Qi Q, Zhang H, Zhang Y, Sun D, Liang P (2019b) Catalytic oxidation of toluene,
1749 ethyl acetate and chlorobenzene over Ag/MnO_2 -cordierite molded catalyst. *Sci Rep* 9:1–10.
1750 <http://doi.org/10.1038/s41598-019-48506-5>
- 1751 Zhu X, Cheng B, Yu J, Ho W (2016) Halogen poisoning effect of $\text{Pt}-\text{TiO}_2$ for formaldehyde
1752 catalytic oxidation performance at room temperature. *Appl Surf Sci* 364:808–814.
1753 <http://doi.org/10.1016/j.apsusc.2015.12.115>